NOTICE

The quality of this microform is heavily dependent upon the quality of the original thesis submitted for microfilming. Every effort has been made to ensure the highest quality of reproduction possible.

If pages are missing, contact the university which granted the degree.

Some pages may have indistinct print especially if the original pages were typed with a poor typewriter ribbon or if the university sent us an inferior photocopy.

Reproduction in full or in part of this microform is governed by the Canadian Copyright Act, R.S.C. 1970, c. C-30, and subsequent amendments.

AVIS

La qualité de cette microforme dépend grandement de la qualité de la thèse soumise au microfilmage. Nous avons tout fait pour assurer une qualité supérieure de reproduction.

S'il manque des pages, veuillez communiquer avec l'université qui a conféré le grade.

La qualité d'impression de certaines pages peut laisser à désirer, surtout si les pages originales ont été dactylographiées à l'aide d'un ruban usé ou si l'université nous a fait parvenir une photocopie de qualité inférieure.

La reproduction, même partielle, de cette microforme est soumise à la Loi canadienne sur le droit d'auteur, SRC 1970, c. C-30, et ses amendements subséquents.

Canada

Local Optic Adaptive Distribution

Fakher Ayadi

A Thesis

in

The Department

of

Electrical and Computer Engineering

Presented in Partial Fulfillment of the Requirements

for the Degree of Master of Applied Science at

Concordia University

Montreal, Quebec, Canada

December, 1990

ISBN 0-315-64648-9

ABSTRACT

Local Optic Adaptative Distribution

Fakher Ayadi

A technique for utilizing optical fiber in a local environment is described. The unique feature of the technique is that it has the ability to adopt to changing traffic loads by changing the connectivity between stations.

In order to do this, a general structure, ShuffleNet, serves as the logical overlay on a physical structure such as the star coupler. The work is predicated on the development of appropriate devices such as an optical amplifier.

This concept is supported by performance curves which show an optimum logical configuration for each value of traffic load in the network, and for two different cases. In the first case there is no restriction on the bandwidth of optical amplifiers, and the second case with a bandwidth restriction on the optical amplifiers.

ACKNOWLEDGEMENT

I would like to express my deep gratitude to my thesis supervisor Dr. J. F. Hayes for his invaluable assistance and constant guidance throughout this research, and for his advice and constructive criticism during the preparation of this thesis.

I would also like to express my appreciation to the University Mission of Tunisia for its support throughout my studies.

Table of Contents

LIST OF PRINCIPAL SYMBOLS

a : core radius

c : light velocity

f : frequency

k : the number of columns in the ShuffleNet

n : refractive index

n^* : number of modes

$\bar{n}_D$: the expexted queue length for the higher priority traffic

B : the total bandwidth used by one source

C_w : bit rate per wavelength

C_L : the capacity per link

D : dispersion

D_1 : the higher priority delay

D_2 : the lower priority delay

D_p : the processing delay

D_M : the multiplexing delay

D_T : the total delay

$E[L]$: the expected queue length for the lower priority traffic

F : the number of optical amplifiers needed to cover the network

G : the number of users sharing the same optical amplifier

$G_{(1)}(z)$: the higher priority generating function

$G_{(2)}(z)$: the lower priority generating function

$\bar{H}$: the expected number of hops

L : the number of links in the ShuffleNet

M : the multiplexing factor

M^* : the power margin

N : the total number of stations

P : the number of arcs going out from each station

$P_T(k)$: input power at the input port

S : dispertion slope

T : slot duration

T_F : frame duration

V_g : group velocity

W : W the total number of physical channels

λ : the amount of traffic destinated for each station

λ^* : free space optical wavelength

λ_{local} : the locally generated traffic per link

Δ : the number of wavelengths covered by each optical amplifier

$\Delta\lambda^*$: spectral width of the source

Λ : the total amount of traffic on each link

Λ^* : the spectral bandwidth

Λ' : the traffic generated by one source

Λ_T : the through traffic

List of Figures

List of Tables

CHAPTER ONE

INTRODUCTION

Optical fiber has become the preferred transmission medium for telecommunications. By virtue of its low attenuation properties, single mode optical fiber has emerged as the technology of choice for point-to-point communication applications. Attention has begun to shift toward the application of this lightwave technology in Local Area Network (LAN) and Metropolitan Area Network (MAN) implementation. Here, the appeal of the technology is its huge bandwidth potential: thousand of GHz are available [2].

Barring an unforesen technological breakthrough we do not expect to see the implementation of ideal lightwave networks in the near future, so we are forced to deal with hybrid networks that employ a combination of both optical and electronic technologies as shown in Figure 1.1. A fundamental constraint on the architecture of a lightwave network is the electro-optic bottleneck, or the inability to electro-optically modulate or demodulate light over a bandwidth greater than a few GHz, only a tiny fraction of the optical bandwidth. Thus to tap the bandwidth of the medium, we must consider techniques in which the bandwidth can be split up into channels that are speed compatible with the digital devices attached to the optical fiber. One such approach, called Wavelength Division Multiplexing (WDM) could provide a large number of high-speed (e.g., 1 Gbits) channels on a single optical fiber by independently modulating different wavelengths of light in the spectrum passed by the fiber.

The multichannel multihop lightwave network or ShuffleNet [3, 11] is one such architecture, which has been advocated for use as a MAN, supporting thousand of users spread over a geographical region with a radius of up to 100 kilometers (Km). By using a large collection high-capacity WDM channels for concurrent message transmission,

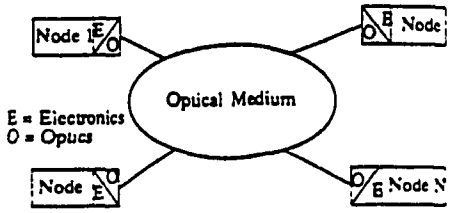

Figure 1.1. Hybrid Lightwave Network.

ShuffleNet can achieve an aggregate throughput far in excess of that achieved by more conventional single-channel MANs such as the Fiber-Distributed Data Interface (FDDI) and Distributed Queue Dual Bus (DQDB) networks [32].

The multihop network consists of a physically distributed optical topology, and traffic generating and terminating nodes, each of which has been allocated some small number of transmitters and receivers. Wavelengths are assigned to these transmitters and receivers, creating several independent channels all of which are wavelength multiplexed onto the optical medium (Figure 1.1), and define the logical connectivity (ShuffleNet) among the nodes. For a given source-destination pair a message may have to hop through several intermediate nodes, or equivalently over different wavelengths, before reaching the destination.

The logical interconnection pattern originally proposed is consisted of several stages connected through a perfect Shuffle, the last stage being connected back to the first stage as if the entire graph were wrapped around a cylinder [3, 11]. For large a number of users there are a lot of possibilities for arranging N depending on the choice of the number of stages. So, the ShuffleNet logical pattern is general in that it may assume any one of a large number of forms.

The key property of the multihop scheme turn out to be the relative independence between the logical interconnection pattern among nodes and the physical topology or fiber layout. Among all possible physical topologies, we mention the bus topology, the tree topology, the star topology, and all combinations of these topologies (example: the tree star tree topology).

By deploying optical transmitters and receivers that can be slowly tuned to any of the wavelengths in use, it becomes possible to adapt several logical connectivities among the nodes to variations in traffic with the same given physical topology. The reconfiguration is under the control of a single parameter, the connectivity. Besides

using WDM, a second parameter, called the multiplexing factor, specifies the number of Time Division Multiplexed (TDM) channels that share a single wavelength.

Our work involved a study of performance, in term of message delay, for a range of connectivity and multiplexing factors, for the ideal case of unlimited bandwidth optical amplifiers and for the case of optical amplifiers with a bandwidth constraint.

CHAPTER TWO

OPTICAL COMPONENTS

In this chapter we will discuss a number of fiber optic components, and transmission and detection methods that can be used to implement our network. First, we review the characteristics of fiber optic components used in the construction of the transmission medium. Then, we explain the difference between coherent and direct detection.

2.1 Fiber-Optics Components

2.1.1 Optical Fiber

The transmission of optical signals via optical fibers was first proposed by Kao and Hocklam [18] in 1966. At the beginning, the losses or attenuation in fibers were in excess of 1000 dB/km. However, after a great deal of research, the current excess loss has been reduced to 0.2 dB/km [19]. This low loss together with high bandwidth is the basis for the current interest in fiber as a transmission medium.

2.1.1.1 Ray Theory

The transmission of light in optical fiber can be explained by the ray theory of light propagation. This theory is based on the approach that considers light as a narrow ray. These rays obey a few simple rules.

(1) In vacuum, rays travel at a velocity, $c = 3\text{x}10^8$ m/sec. In any other medium, rays travel at a speed given by the relation, $v = c/n$.

Where

n: is the refractive index of the medium

c: is the velocity of light in vacuum.

(2) Rays travel in straight paths unless deflected by some change in the medium.

(3) When a light ray hits a boundary between two media, a ray reflects at angle equal to the angle of incidence, i.e.,

$$\theta_i = \theta_r$$

Where θ_i is the angle of incidence and θ_r is the angle of reflection.

(4) If a light ray crosses a boundary, the angle of refraction θ_t is given by Snell's law

$$\frac{\sin\theta_t}{\sin\theta_i} = \frac{n_1}{n_2} \tag{2.1}$$

where θ_t is the angle of transmission, and n_1 and n_2 are the refractive indices of the incident and transmission regions, respectively. This is shown in Figure 2.1.

2.1.1.2 Total Internal Reflection

If a light ray is incident at a boundary in which medium 1 has a higher refractive index than medium 2, as the angle of incidence θ_i is increased, a situation is attained in which the refracted ray points along the surface. The value of refracted angle at which this occurs is 90^o. For angles of incidence larger than this critical angle θ_c there is no refracted ray. This situation gives rise to a phenomenon called *total internal reflection.*

The critical angle is obtained by substituting $\theta_t = 90^o$ in Snell's law

$$n_1\sin\theta_c = n_2\sin 90^0 \tag{2.2}$$

$$n_1\sin\theta_c = n_2 \tag{2.3}$$

$$\sin\theta_c = \frac{n_2}{n_1}. \tag{2.4}$$

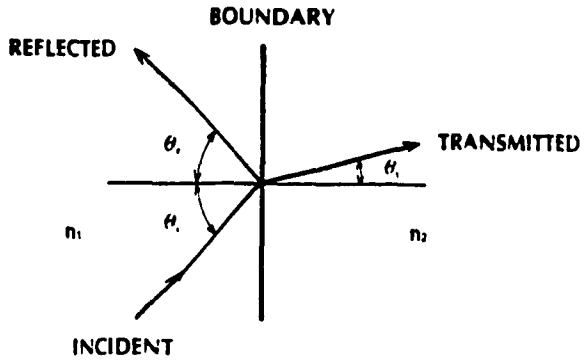

Figure 2.1. Incident, Reflected and Transmitted Rays at Boundary.

Total internal reflection occurs when the angle of incidence is equal to or greater than the critical angle. This is the primary concept in transmitting light energy in fiber optic media.

2.1.1.3 Principles of Propagation in Optical Fibers

Various types of fibers are commercially available for different applications. The optical fiber consist of a core and a cladding as shown in Figure 2.2. This type of fiber is known as step index fiber. It is constructed in such a way that the refractive index of the core is larger than the refractive index of the cladding. Figure 2.3 depicts the propagation mechanism of light energy in the fiber. The optical signal will propagate along the fiber by multiple internal reflections, provided that the angle of incidence θ_i on the core-cladding boundary is greater than the critical angle.

2.1.1.4 Modes in Optical Fiber

When an optical signal is launched into the fiber from the source, all rays having angles between 90^o and the critical angle are allowed to propagate. All the other rays exceeding the critical angle are evanescent waves, i.e., the waves are severely attenuated as they propagate along the fiber. The allowed direction corresponds to the modes of the optical waveguide. The mode is a complex mathematical and physical concept describing the propagation of electromagnetic waves. This concept can be summarized in the following points.

- Each mode corresponds to a specific direction of ray travel and has a unique transverse field pattern.
- The modes are the resonances of the waveguide for ray directions that are inclined with respect to the boundary normal.
- The effective refractive index of a given mode can be found from a mode chart.

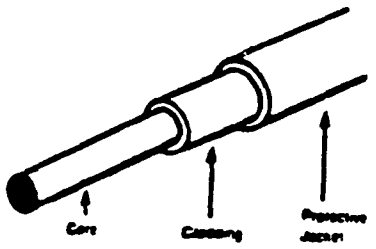

Figure 2.2. Fiber Construction.

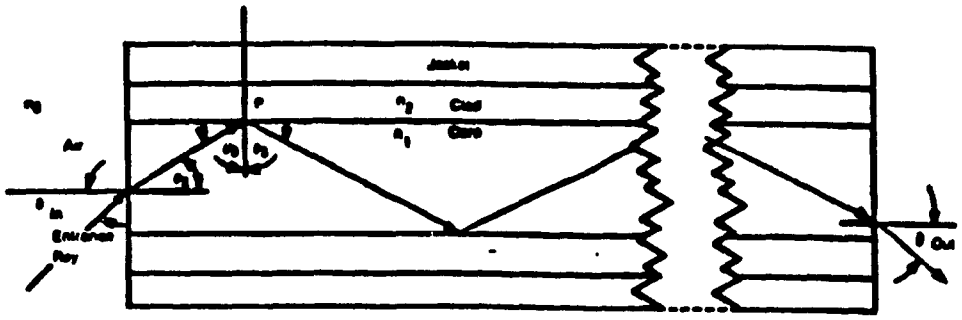

Figure 2.3. Propagation Mechanism of Light Energy within the Fiber.

The longitudinal propagation factor can also be obtained.

- Two orthogonal polarizations exist, denoted as transverse electric and transverse magnetic modes.
- The number of allowed modes increases with core thickness and with the difference in refractive indices between the core and the cladding of the fiber.
- For sufficiently thin core, the optical fiber can support only a single mode. This corresponds to the single mode fiber.

There are two principal types of fibers that are used in optical fiber communications, step index fibers and graded index fibers. These fibers are fabricated by varying the material composition of the core [20]. In the case of step index fiber the refraction index of the core is uniform throughout the fiber except at the core-cladding boundary, as shown in Figure 2.4. At the boundary the refractive index undergoes an abrupt change (or step). Whereas in graded index fiber the core refractive index varies as a function of the radial distance from the center of the fiber [20], as shown in Figure 2.5. Step index and graded index fibers can be further classified into single mode and multimode fibers.

In the single mode fiber, only one mode is allowed to propagate. But in multimode fibers the propagation of optical energy in many modes is allowed as shown in Figure 2.4. The number of modes a fiber can support depends on the physical parameters of the fiber and frequency of the signal to be transmitted. The relation between the number of modes in a fiber and physical parameters of the optical wave guide given by [21]

$$N^* = \frac{2\pi^2 a^2}{\lambda^{*2}}(n_1^2 - n_2^2) \qquad (2.5)$$

Where

N^* : is the number of modes

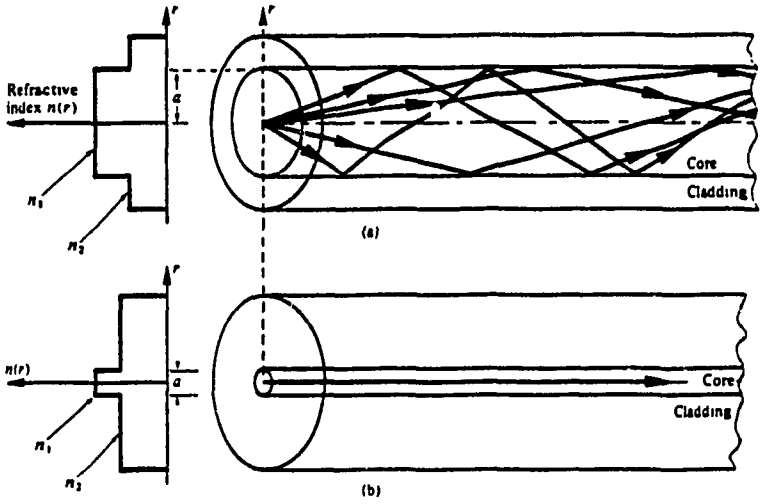

Figure 2.4. Step Index Fibers: (a) Multimode Step Index Fiber; (b) Single Mode Step Index Fiber.

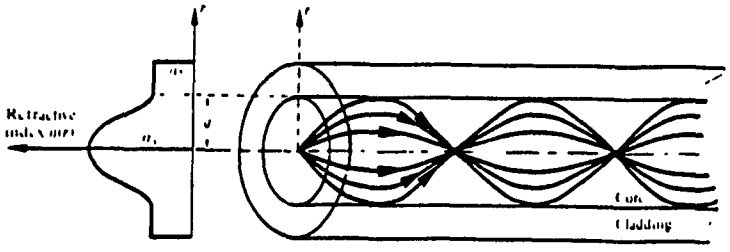

Figure 2.5. Multimode Graded Index Fiber.

a: is the core radius

λ^*: is the free space wavelength

n_1: is the refractive index of the core

n_2: is the refractive index of the cladding

Two sets of standard fiber dimensions:

1) For graded-index multimode fibers, a core diameter of 50 μm and a cladding diameter of 125 μm.

2) For step-index fibers, a core diameter of 200 μm but an unspecified cladding diameter.

3) For single mode fibers, a core diameter of 5 μm.

2.1.1.5 Transmission Characteristics

From a transmission performance point of view, single mode fibers have a clear advantage over any other transmission media including the multimode fibers, as the distance becomes large.

First, the single mode fibers present an attenuation characteristics as typically shown in Figure 2.6, which gives the variation of attenuation with wavelength of the optical signal. The attenuation in the case of single mode fibers is primary caused by the intrinsic Rayleigh scattering of the doped fused silica, which is proportional to the inverse of the 4^{th} power of wavelength. Beyond 1600 nm a rapid increase in the attenuation is due to the intrinsic infrared tail of the material used in the fiber. Other sources of losses can be mentioned such as the Hydroxyl (OH) absorption losses and excess losses caused by waveguide imperfection and metallic impurities. These losses are negligible, and can be eliminated completely in certain cases. For examples, the absorption losses of the Hydroxyl (OH) ion at 1380 nm are zero [2]. For the multimode fibers the attenuation characteristics is shown in Figure 2.7.

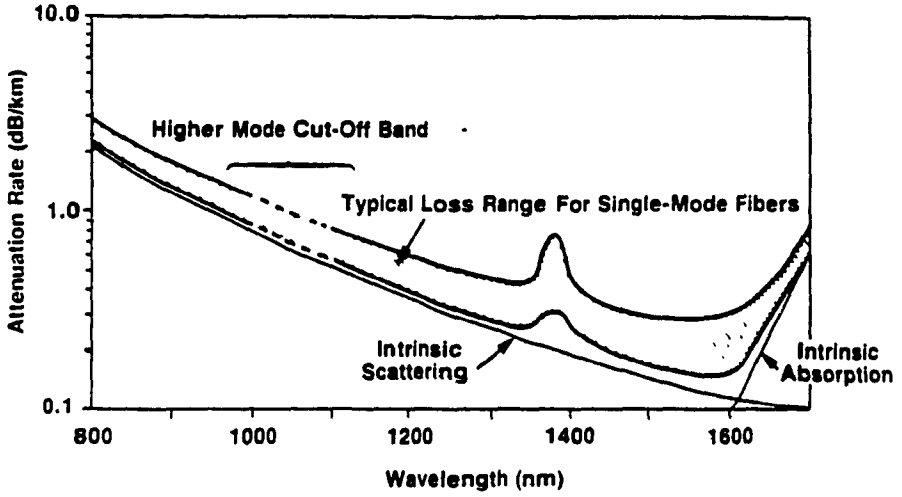

Figure 2.6. Typical Spectral Loss of Single Mode Fibers.

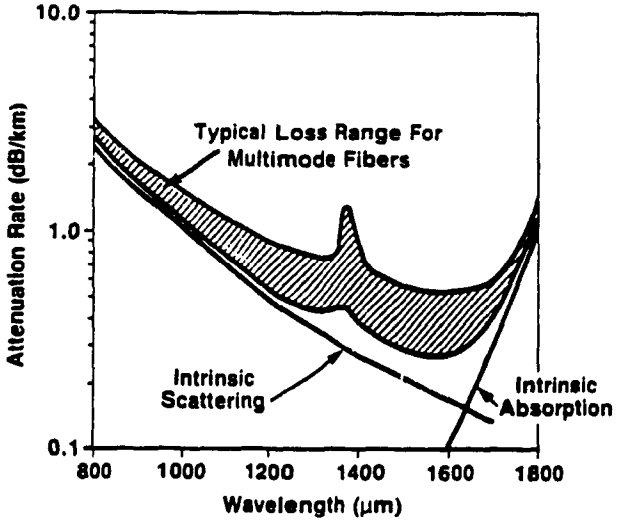

Figure 2.7. Typical Spectral Loss of Multimode Fibers.

Multimode fiber losses have the same fundamental limitations as single mode fibers, however, they are generally higher than those of the single mode fibers because of higher dopant concentrations and a higher sensitivity to microbending losses particularly of the higher-order modes.

2.1.1.6 Dispersion

If a light pulse is launched into an optical fiber, at the receiving end the pulse appears wider. This is due to the dispersive nature of the fiber material, i.e., the refractive index profile of the medium varies as a function of wavelength. As a result, different wavelengths in the spectrum of the source travel at different velocities, thus causing the pulse to spread. The dispersion is usually specified in units of ps/nm-km (pico second/nanometer-kilometer).

The most important consequence of dispersion is the limitation of the capacity of the optical channel. As the light travels along the fiber the pulse broading will cause adjacent pulses to overlap. The resulting interference between symbols is called Inter Symbol Interference (ISI). An example is shown in Figure 2.8.

For the multimode fiber the bandwidth is limited mainly by modal dispertion which is due to the variation in group velocities of the different modes [20]. The group velocity V_g is the speed at which the pulse travels along the fiber. V_g is given by

$$V_g = \left[\frac{d\beta}{d\omega}\right]^{-1} \tag{2.6}$$

where ω is the angular frequency of the wave, and β is the propagation constant along the fiber axis which is equal to

$$\beta = n_1 \frac{\omega}{c} \tag{2.7}$$

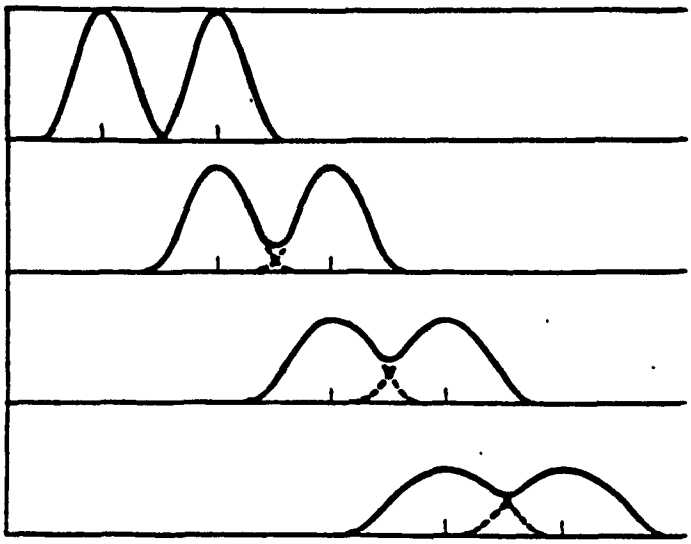

Figure 2.8. Optical Pulses Tend to Overlap as they Travel along the Fiber.

This dispersion can be eliminated for the single mode fiber. Then, the bandwidth for the single mode fiber is limited only by chromatic dispersion.

The chromatic dispersion consist mainly of material and waveguide dispersion

$$D_{ch}=D_{mat}+D_{wvg} \quad (ps/nm.Km). \tag{2.8}$$

In standard single mode fibers, the chromatic dispersion is dominated by the material dispersion, which is primary caused by the fact that the refractive index of the fiber core depends on the wavelength. This dependence is a function of the core dopants, such as fused silica, germanium, and is generally fixed by other considerations. Figure 2.9 shows that for the single mode fiber characterized in Figure 2.6, the chromatic dispersion is almost equal to zero at some wavelengths in the range of 1300 nm. Since the bandwidth of single mode fiber is inversely related to the dispersion, in that range of wavelength ($D_{ch}\approx 0$) the intrinsic bandwidth of the transport medium becomes unlimited for all practical purposes. The only limitation is due to optoelectronics and the electronics.

2.1.1.7 Dispersion vs Bandwidth

An important parameter to be determined is the bandwidth of the optical fiber. Unlike the multimode bandwidth, the bandwidth of a single mode fiber depends on the input source spectral width and on the fiber dispersion. As we see above the dispersion can be equal to zero and then the bandwidth of the single mode fiber would seem to go to infinity at this value. However, the dispersion slope is the factor that limits the bandwidth to finite values.

The bandwidth can be given by [1]

$$BW \le \frac{1}{4}[2(DL\Delta\lambda^*)^2+(SL(\Delta\lambda^*)^2)^2]^{-0.5} \tag{2.9}$$

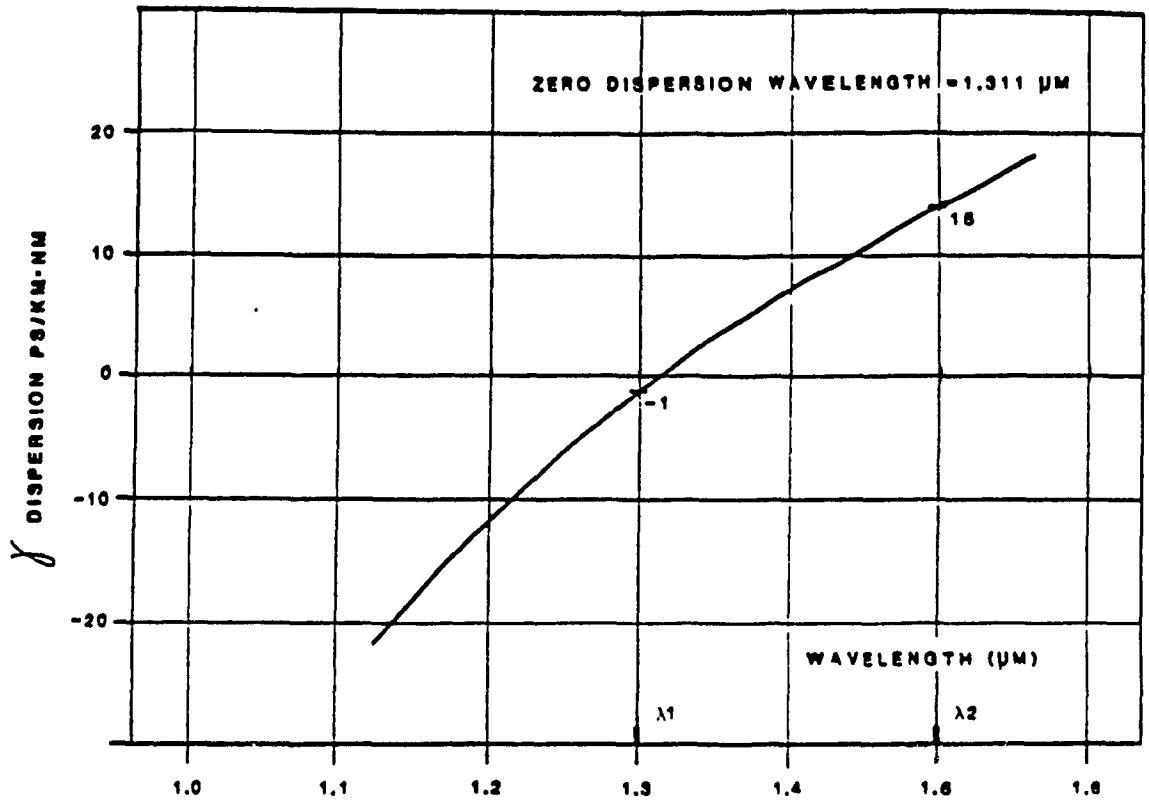

Figure 2.9. Chromatic Dispersion for the Single Mode Fibers.

Where

S : is the dispersion slope at the wavelength of interest.

D : is the dispersion.

L : is the fiber length.

$\Delta\lambda^*$: is the spectral width of the source.

From this equation, we notice that near zero dispersion wavelength the bandwidth is a function of the dispersion slope since $D \approx 0$, but at wavelengths away from λ_0 the bandwidth is a function of the dispersion since D >> S.

2.1.1.8 Properties and Impact of the Optical Fiber

Single mode fiber has become the preferred transmission medium for telecommunications, because of its unlimited transmission bandwidth over very long, unrepeatered distances. The single mode fiber propagation exhibits low dispersion of the transmitted pulse [21], and this kind of fiber does not suffer from intermodal dispersion.

Furthermore, single mode fiber has two low-loss regions near 1300 nm and 1500 nm, and offers enormous transmission bandwidth: thousands of GHz are available [2] as shown in Figure 2.10. It is within the realm of possibility that one single mode fiber can provide one thousand of individual wavelengths, each carrying information over hundreds of kilometers at Gigabit rates. These advantages make the use of single mode fibers very attractive for Metropolitan Area Network (MAN) implementation.

Multimode fiber is preferred to single mode fiber for low bandwidth and low transmission distances such local loops and telephony and Local Area Networks (LAN), which have less need for high performance because of the distance. Multimode fibers and LEDs have been used in LANs operating at rates ≤ 100 Mbps. Since multimode fibers have a larger core diameter than single mode fibers, it is easier to launch optic power from an LED into a multimode fiber than a single mode fiber.

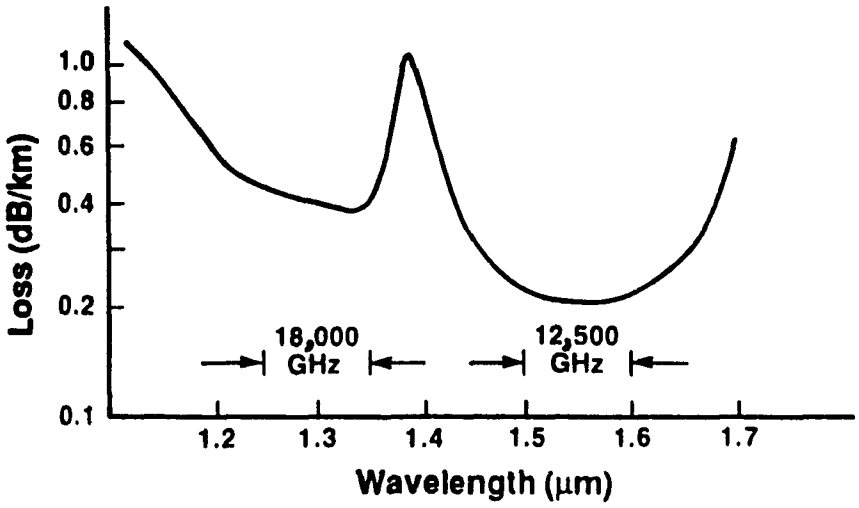

Figure 2.10. Single Mode Fiber Bands.

The single mode fibers are always excited with Laser diodes because of their narrow core diameter.

At the same time single mode fiber presents certain limitations. The bandwidth of a single mode fiber can be limited by fundamental energy considerations. Consider the simple point-to-point optical link shown in Figure 2.11, consisting of a transmitter coupled to a receiver via a lossless fiber. To detect a transmitted bit, the receiver requires a minimum amount of optical energy, E. In the ideal case, E is independent of bit rate, so operation of the link at a rate B requires a power level of EB at the receiver. We conclude that for a transmitter with output power P, the maximum (power-limited) transmission rate is P/E. This power problem makes it difficult to translate many high-capacity networking concepts into practical photonic implementations. For example, the absence of amplification will place a limit on the splitting that can take place for a given physical topology due to the power problem.

Although photonic technology is capable of supporting many Tb/s of throughput, the digital electronic components at the nodes of the lightwave network, which typically operate at rate of 1 Gb/s or less, can drastically limit total throughput. This situation is the electronic bottleneck [22], mentioned earlier.

2.1.2 Optical Sources

The principal optical sources used in fiber optic communication systems are Laser diodes and Light Emitting Diodes (LED). The operation of these two sources are dealt with in the following sections.

2.1.2.1 Light Emitting Diodes (LED)

The LED consist of a semiconductor pn junction, which emits light when forward biased. The operation of this device can be explained by band theory. Referring to Fig-

ure 2.12, the two bands with energy gap E_g are the conduction band and the valence band. In the conduction band, the electrons are loosely bounded to the atoms and are ready available for conduction. In the valence band, the holes (positively charged) are free to move. Holes are locations at which an electron is taken away from neutral atom; as a result, the atom is positively charged. A free electron can recombine with a hole, returning the atom to its neutral state. Energy is released when this occurs. The amount of energy radiated is given by [23,24].

$$E_g = hf \tag{2.10}$$

Where

E_g: is the difference in energy between conduction band and the valence band.

f: is the frequency of radiation

h: is the Planck's constant

A p-type semiconductor has excess holes and n-type semiconductor has excess electrons. When p-type and n-type materials are brought together an energy barrier is formed as shown in Figure 2.12. Normally, the electrons in the conduction band do not have sufficient energy to cross the barrier and produce a photon. When the junction is forward biased, the barrier decreases; consequently, the electrons and holes have sufficient energy to cross the barrier and recombine to produce a photon. In essence, radiation from an LED is caused by recombination of holes and electrons under the influence of externally applied voltage [23,24].

As seen from the equation of the radiated energy, the frequency of radiation varies with the band gap energy (E_g), consequently, the material used for fabrication. Table 2.1 lists various types of LEDs that are used in fiber optic communications.

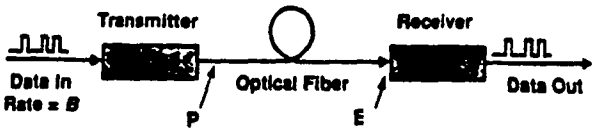

Figure 2.11. Point-to-Point Lightwave Link.

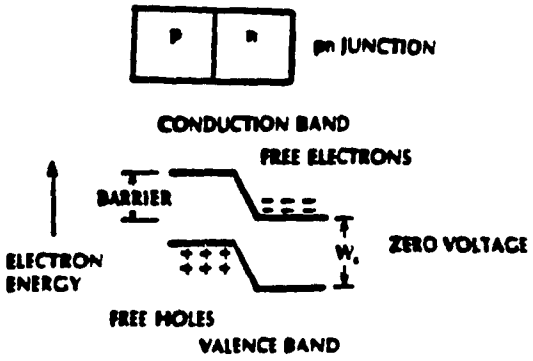

Figure 2.12. Band Structure of pn Junction.

Table 2.1 Various Types of LEDs Used in Fiber Optic Communications [30].

Material	Wavelength Range μm	Bandgap Energy ev
GaAs	0.9	1.4
AlGaAs	0.8-0.9	1.4-1.55
InGaAs	1.0-1.3	0.95-1.24
InGaAsP	0.9-1.7	0.73-1.35

2.1.2.2 Lasers

Laser is the abbreviation for *light amplification by stimulated emission of radiation.* The medium for lasing can be a gas, a liquid, a crystal or a semiconductor [25]. For optical communications the Laser sources employed are semiconductors. Laser action is the consequence of three processes [25]. These are photon absorption, spontaneous emission, and stimulated radiation. These are depicted by the energy level diagrams shown in Figure 2.13. E_1 is the ground level energy and E_2 is the excited state energy. In accordance with Plank's law, transition between these two states involves the absorption or emission of a photon of energy, $hf = E_2 - E_1$ [25]. Usually the atom is at ground state. When a photon of energy $E_2 - E_1$ collides with the atom, an electron in state E_1 can absorb the photon energy and be excited to state E_2 as shown in Figure 2.13. Since the electron is in an unstable state, it will eventually return to ground level emitting a photon of energy equal to the difference $E_2 - E_1$ [25]. This occurs without any external stimulation and is called spontaneous emission. It is possible for an electron to make the downward transition from the state E_2 (the excited state) to E_1 (to the ground level) by an external stimulation as shown in Figure 2.13 c.

In selecting a LED or a Laser diode as a source there are certain advantages and disadvantages for each type of device. Some of the advantages of a Laser over an LED are [18,25]:

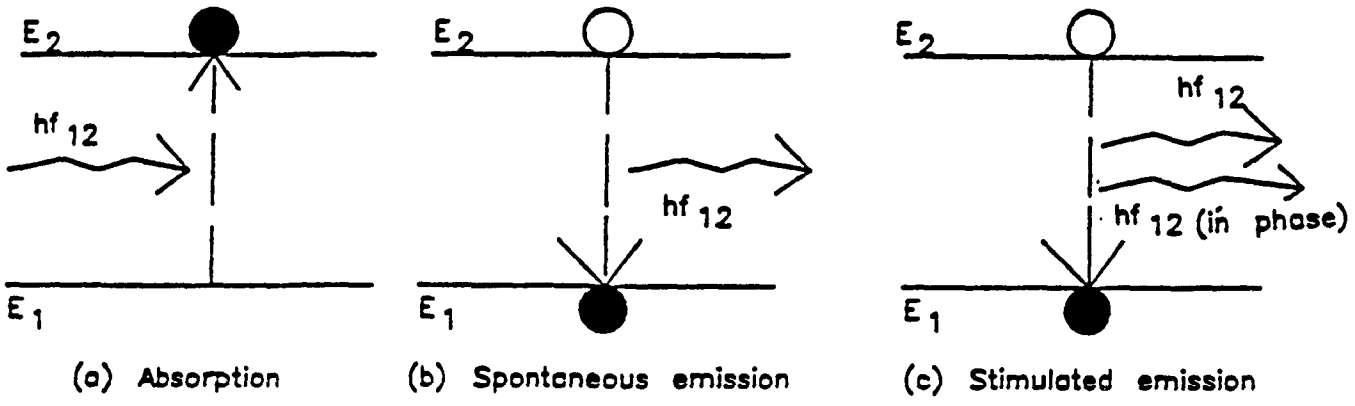

Figure 2.13. Energy Level Diagram in Lasers.

a) A faster response time. This implies faster data transmission rates are possible.

b) The spectral width of a Laser is narrow, which implies less distortion due to dispersion.

c) The optic power that can be coupled from a Laser is greater, consequently, greater transmission distance is possible.

Some of the disadvantages of Lasers are:

a) Fabrication of Lasers is more complicated.

b) The optical output is strongly dependent on temperature. As a result, the transmitter circuitry is more complicated than for the LED transmitter.

c) The Lasers are very expensive compared to LEDs.

The major difference between LEDs and Lasers is that the power emitted from an LED is incoherent, whereas that from a Laser is coherent. In a coherent source the optical power is generated in an optical resonant cavity. The optical power emanated from this cavity is highly chromatic and the output beam is very directional. In an incoherent source such as an LED no optical cavity exists for wavelength selectivity, consequently the output radiation has broad spectral width. The coherent optic power from Laser can be coupled into single mode or multimode fibers. However, the optical power output from an LED because of its incoherency can only be coupled into a multimode fiber [25].

The choice of a particular optic source depends on many factors. As an aid in selecting a particular diode for fiber optic communication, the characteristics of optical sources are summarized in Table 2.2.

Table 2.2 Typical Characteristics of Diode Light Sources [30]

Property	LED	Laser Diode	Single Mode Laser Diode
Spectral width (nm)	20-30	1-5	<0.2
Rise time (ns)	2-250	0.1-1	0.1-1
Modulation bandwidth (MHz)	< 300	< 2000	2000
Coupling efficiency	very low	moderate	moderate
Temperature sensitivity	low	high	high
Circuit complexity	simple	complex	complex

2.1.2.3 Wavelength Tunable Lasers

Having reviewed the case of single-frequency Laser, we will now discuss the case of wavelength tunable Lasers. Wavelength tuning can be achieved by providing a frequency tunable loss element inside the laser cavity. But the most common method is to use a diffraction grating in an external cavity.

The tuning range of a grating-loaded external cavity Laser is limited, in principle, only by the width of the gain spectrum of the semiconductor material employed as the gain medium in the Laser. For InGaAsP material, a maximum tuning range of 55 nm has been achieved [26]. While this large tuning range is desirable, tuning must be done mechanically. Electronically tunable external cavity Lasers using either an Electro-Optic filter or an Acousto-Optic filter are more attractive. However, neither method can provide continuous wavelength tuning over a useful range.

Table 2.3 presents a comparison of the major wavelength tunable Lasers in term of relevant system parameters.

Table 2.3 Wavelength Tunable Semiconductor Lasers [31]

Configuration	Tuning Method	Tuning Range
Grating Tuned External Cavity Laser	Mechanical	55 nm (d)
Electro-optically Tunable Laser	Electronic	7 nm (d)
2-Sectioned DBR Laser	Electronic	3.3 nm (c)
3-Sectioned DBR Laser	Electronic	2 nm (c)
PIN Tunable Laser	Electronic	21 nm (c)

Note: (d) discrete tuning, (c) continuous tuning.

2.1.3 Optical Receivers

The building blocks of an optical receiver are shown in Figure 2.14. They consist of a photodetector, preamplifier, main amplifier, equalizer, and threshold logic. The most important block shown in Figure 2.14 is the photodetector.

2.1.3.1 Optical Detectors

The purpose of this device is to convert an optical signal to electrical signal. The signal is then amplified and processed further. If the chosen detector has good characteristics, such as linearity and responsivity, the requirements on the rest of the signal processing circuitry are less stringent. The two main photodetectors used in optical fiber communications are silicon positive-intrinsic-negative (PIN or p-i-n) photodiodes and Avalanche photodiodes (APD).

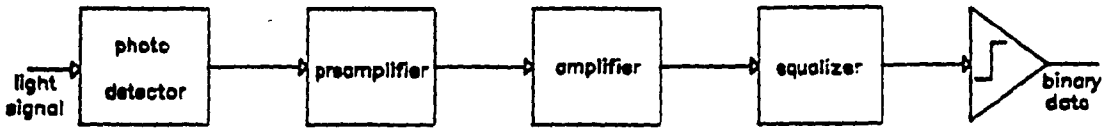

Figure 2.14. Optical Receiver Block Diagram.

2.1.3.1.1 PIN Photodetectors

PIN photodetectors are the most common type of detectors employed in optical fiber systems. Its configuration and biasing arrangement is shown in Figure 2.15. The device structure consists of p and n regions separated by lightly doped n-doped intrinsic (i) region. For normal operation the device is reverse biased. In the pn junction, the carriers drift randomly with relatively low velocities [24]. As a result, the displacement current produced by a hole-electron pair occurs as a pulse of short duration when the carriers are moving through the depletion region [24]. The response due to the optical power incident on the detector in the depletion region is immediate. However, the electron-hole pairs generated in diffusion region produce a delayed response [24]. To increase the speed of the device, it is necessary for the depletion region to enclose the absorption region [18]. A method to increase the absorption region is to increase the reverse bias voltage or by decreasing the impurities (doping) in n-type material.

2.1.3.1.2 Avalanche Photodetectors (APD)

In the ideal situation, for PIN diode, if every incident photo produces a hole-electron pair, then at wavelength of $1\mu m$, the responsivity is about 0.8 A/w [24]. Most of the receivers operate with input power levels as low as few nano watts. Thus, with PIN detectors, the photocurrent generated would be very small in the order of few nano amperes. Such small current would be severely corrupted by the amplifier noise. To increase the number of electron-hole pair generated for each incident photon an avalanche photodiode is used. The structure is shown in Figure 2.16.

Avalanche photodiode has high electric field region (avalanche region). In the avalanche region, carriers move randomly and occasionally collide with ions, thereby, producing new carriers. The newly created carriers gain sufficient velocity, thus producing some more carriers. This phenomena is called the avalanche effect [20].

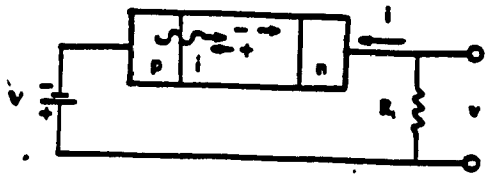

Figure 2.15 PIN Photodetector.

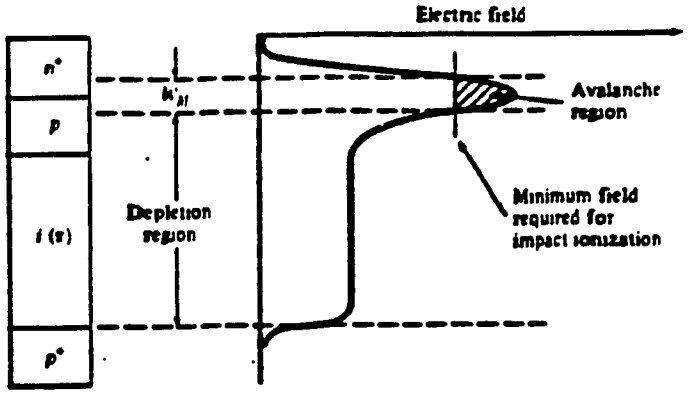

Figure 2.16 APD and its Electrical Field Profile.

This avalanche effect multiplies the primary photo current by a random gain factor, thereby increasing the effect responsivity of an APD by a random gain factor G_r. As a result, the receiver sensitivity is also increased.

The carrier multiplication achieved by this method causes noise, since the gain factor is random [24]. This randomness in the avalanche process produces an effective noise which limits the receiver sensitivity of the APD devices. However for a certain range of gain factor, the effective noise of the APD is less than that produced by amplifier noise; consequently, the APD offers significant benefits over the PIN detector [24]. The typical characteristics of PIN and APD's are shown in Table 2.4.

Table 2.4 Typical Characteristics of Junction Photodetector.

Material	Structure	Rise time ns	Wavelength nm	Gain
Silicon	PIN	0.5	300-1100	1
Germanium	PIN	0.1	500-1800	1
InGaAs	PIN	0.3	1000-1700	1
Silicon	APD	0.5	400-1000	150
Germanium	APD	1	1000-1600	50

2.1.4 Optical Amplifiers

In future optical networks, optical amplifiers will be required to assure adequate reception among all users, and to increase the total number of users in the network. When the number of users gets large, the dividing losses in the star couplers or splitters, tap, filter and line losses severely limit the power margin. These losses can be made up by optical amplifiers. One of the most promising candidates is the traveling wave semiconductor amplifier shown in Figure 2.17. As an optical wave propagates through the structure, it grows because of stimulated emissions from free carriers in the active region. Each emission event adds coherently to the existing field, so the traveling wave retains

the phase and polarization characteristics of the original signal, while growing in magnitude. The antireflection coating eliminates feedback and, therefore, the possibility of oscillation. Net gain (fiber in / fiber out) is in the vicinity of 20 dB over a 2,500 GHz (20 nm at $\lambda^* = 1.5$ μm) band with a saturation output power greater than 1 mW. Other methods that use an optical fiber doped with erbium ions and pumped by a suitable semiconductor laser, as shown in Figure 2.18, can produce gain within a band (1,520 - 1,550 nm) fixed by the rare-earth ion and the glass used for construction of the fiber [22]. Suitable diode laser pumps at 665, 807, or 1,480 nm, with power levels sufficient to provide gains of 20 dB and saturation output above 1 mW, are expected to be commercially available very soon.

There are three characteristics of an optical amplifier that limit its usefulness in LAN application: maximum output power and internal noise generation [22]. The maximum power available from an amplifier is limited by the number of free carriers available for stimulated emission, just as in a Laser. For the usual case of amplifiers based on the same device structures as typical Lasers, we can expect to get only about the same peak power from the amplifier as from a Laser based on the same structure would have given. That is, transmitters and amplifiers deliver roughly equal levels of output power.

In addition to boosting the desired signal, an amplifier adds a background of noise, whose origin is the inevitable spontaneous emission that accompanies all stimulated emission processes. Consequently, as the signal propagates through the amplifiers its signal-to-noise ratio deteriorates, eventually becoming so poor that the desired signal cannot be detected with an acceptably low bit error rate.

Finally, one of the most difficult problems related to optical amplifiers is the bidirectional nature of the gain provided. Any reflection can cause instabilities. Therefore, a nonreciprocal device must be incorporated with the amplifier.

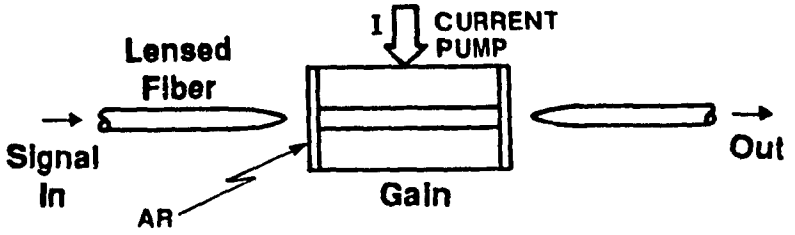

Figure 2.17. Semiconductor Diode Splice Amplifier.

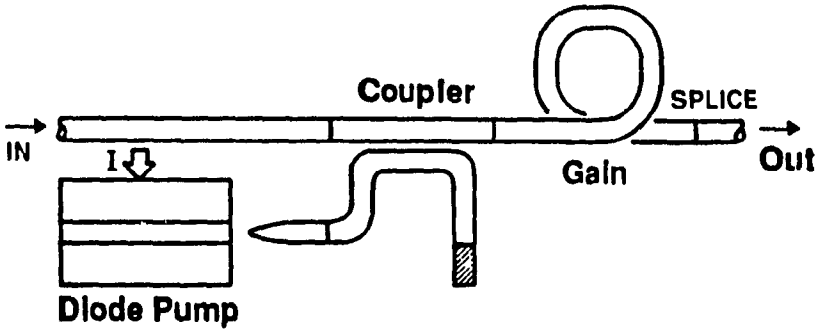

Figure 2.18. Rare-Earth Doped Fiber Amplifier.

2.1.5 Wavelength-Tunable Optic Filters

Optical systems based on space division, time-division, and wavelength-division processing have been extensively investigated. In particular, for wavelength (or frequency) division multiplexing techniques the frequency-tunable filters are key components to provide more functionality.

Frequency-tunable filters are involved in most systems based on "broadcast and select" principle. The basic ingredients in systems using this principle are : N laser transmitters with different center frequencies, a passive star to broadcast every input signal to all the output lines, and finally S_r tunable filters are required to select the desired channels at each output.

An important parameter for the frequency tunable filter is the tuning range. This is illustrated in Figure 2.19. This parameter is important because it limit the maximum number of channels. In particular, the maximum number of channels is given by the ratio of the total tuning range to the channel spacing necessary for minimum crosstalk degradation. For a given channel bandwidth B, the necessary channel spacing varies between 3 and 10 times B, depending on the filter lineshape. For example, for 1 GHz filter bandwidth, 5 GHz channel spacing, and 200 GHz tuning range (equivalent to 1.5 nm around the wavelength of 1.5 μm, and 1.1 nm around 1.3 μm) implies a system capacity of 40 channels. At the receiving point the number of receivers will depend on the available power budget. When using optical amplifiers this will increase the importance of the power budget issue, and increase the maximum number of receivers.

The tunable range and the tuning speed of the tunable filter are determined by the technology used. Table 2.5 [27] presents a comparison of the major frequency tunable filter technologies, Fabry-Perot, Acousto-Optics, Electro-Optics, and semiconductors in term of relevant system parameters.

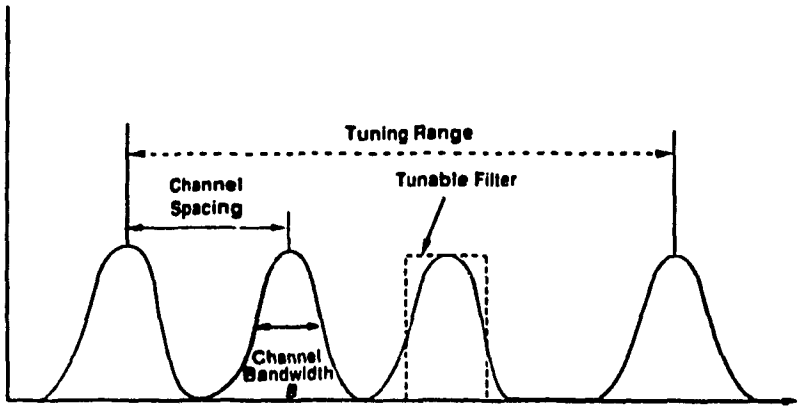

Figure 2.19. Multi-Channel Spectrum and Selection via Tunable Filtering.

Except for bulk Fabry-Perot filters and acousto-optic filters, most of the filter technologies were developed very recently, and further development effort is required to bring these technologies into the hands of commercial manufacturers and system designers.

Table 2.5 Tunable Filters Characteristics

Technology	Fabry-Perot	Acousto-Optics	Electro-Optics	Active Semiconductors
Tuning Range (nm)	50	400	10	1-4
Bandwidth (nm)	<0.01	1	1	0.05
Number of Channels	100s	100s	10	10s
Loss (dB)	5	5	5	0
Tuning Speed	ms	μs	ns	ns
Applications	Video Broadcasting	Video Broadcasting and Circuit Switching	Cross-connect of Few High-Speed Channels	Packet and Circuit Switching

2.1.6 The Passive Star Coupler

An NxN passive optical fiber star is illustrated in Figure 2.20. In the ideal case all N input and N output ports are equivalent. If $P_T(k)$ is transmitted by station k, then $P_T(k)/N$ will appear at each of the output ports (and none of the input ports) and will be broadcast to all stations, including k, equally. In practice, of course, the power division may not be equal and the output distribution may vary with the input port. Several methods are used to built an NxN star with large N. For the case of $N = 2^L$ and L is an integer, a 2x2 star can be used as a building block to construct large N-stars. Figure 2.21 shows 16x16 star coupler that is made by cross-connection of 32 2x2 star couplers. For the general case an NxN star, with N equaling a power of two, requires $\log_2(N)$ stages, each containing (N/2) 2x2 stars, for a total of (N/2) $\log_2(N)$ 2x2 stars [4]. Since the excess loss suffered by a signal propagating through the structure is proportional to the number of stages that is traversed, this lead to a logarithmic behavior of the excess loss.

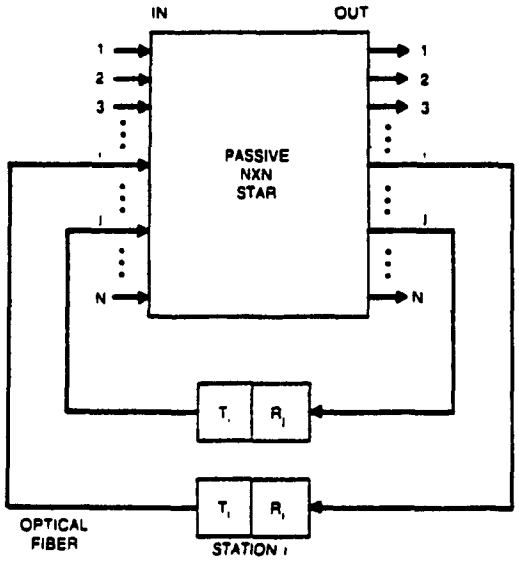

Figure 2.20. The NxN Star with N Optical Input and N Output Ports.

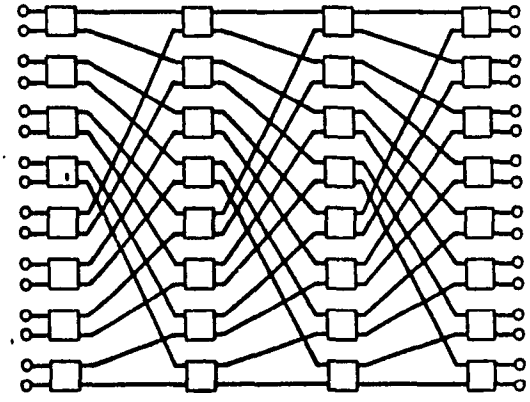

Figure 2.21 A 16x16 Star Made of 32 2x2 Stars.

A simpler method for fabrication of a star with large N is shown in Figure 2.22. It utilizes a planar input waveguide array that radiates into a planar 'free-space' region, which is sufficiently long that the output array aperture is in the far field [5]. If any input guide is excited, it couples energy into the adjacent waveguides in such a way that the far-field is nearly uniform over the N output guides. This structure, shown in Figure 2.22, can support up to 1000 stations (N =1000) for a power margin of 40 dB [6]. The advantages of this structure over the composite structure are that it has only 3 cm in length and it does not require the $N\log_2(N)$ fiber splices of the composite structure (100000 for a 1000x1000 coupler) for an excess loss of the same order [6]. At the same time we mention that a 19x19 star coupler using this method has been built and the power transfer between the arrays is accomplished through radiation in the dielectric slab with theoretical efficiency exceeding 30% under optimized conditions [5].

2.2 Wavelength and Frequency Division Multiplexing

Due to the electronic bottleneck [22] limiting the peak transmission rate to approximately 1 gigabit per second (Gbps), we can not effectively utilize the enormous bandwidth potential of the optical systems, which have the ability to carry several terabits of information per second. For this reason, we consider techniques in which the bandwidth of an optical fiber can be split up into channels that are compatible in speed with the digital devices attached to the optical fiber. One such approach, called Wavelength Division Multiplexing (WDM), could provide a large number of high-speed (e.g., 1-Gbps) channels on a single optic fiber by independently modulating different wavelengths of light in the spectrum passed by the fiber. The system capacity is limited by the number of wavelengths that can be used, up to 1000 wavelengths per fiber. When WDM is used, the available spectral bandwidth Λ^* is divided into W segments. An optical carrier at wavelength λ_k^* is located at the center of each segment and adjacent carriers are separated by Λ^*/W.

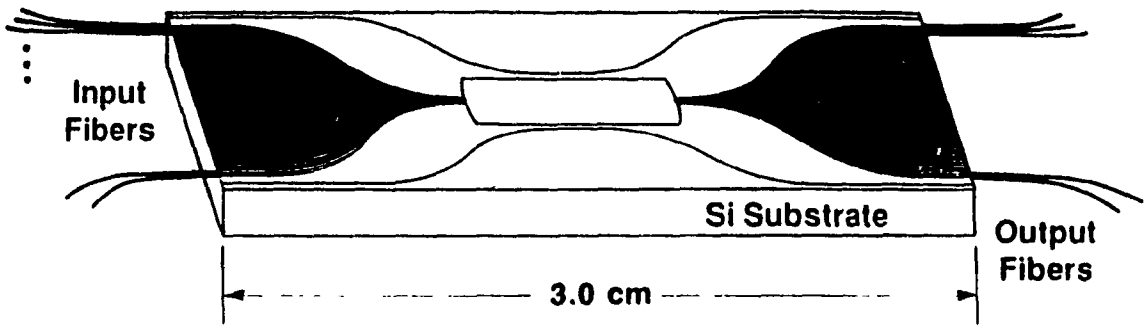

Figure 2.22. Integrated NxN Star.

Since optical sources have been traditionally described in terms of wavelength, it is customary to speak of WDM. From the engeneering standpoint, however, it is simple to deal with optical frequencies. Thus with c the velocity of light in vacuum, $f_k = c/\lambda_k^*$, and increments in frequency are given by

$$\frac{df}{d\lambda^*} = -\frac{c}{\lambda^{*2}} = \left\{180GHz/nm \ @1.3\mu m,\ 125GHz/nm \ @1.55\mu m\right\} \qquad (3.19)$$

If the channel spacing frequency f_c is large compared with the channel bit-rate B ($f_c \approx 15B$) we will speak of WDM. A more efficient but more daunting engineering approach is to reduce f_c to the limit set by interchannel interference. We denote this case Frequency Division Multiplexing (FDM), implying that f_c and B are of the same order ($f_c \approx 6B$). The comb of optical carriers for the case of FDM is shown in Figure 2.23, where the carriers are spaced apart by Λ^*/W, or equivalently F/W, with $F = c\,\Lambda^*/\lambda^{*2}$. The spacing F/W might be six times the terminal bitrate, B.

Various other methods are employed to share the transmission medium on a statistical basis, among these we mention Time Division Multiplexing (TDM), and Code Division Multiplexing (CDM).

2.2.1 Time Division Multiplexing

Time Division Multiplexing (TDM) is generally the preferred means for sharing an optical channel. Hence for MANs a promising approach is let a large number of bursty users to share a smaller number of wavelengths. When TDM is used, a frame of duration MT is divided into M time slots of duration T, as illustrated in Figure 2.24. Each interconnection from one station to another is assigned a particular time slot by a central controller. The transmitter sends a pulse in that time slot at the frame rate F=1/MT and the receiver selects that time slot.

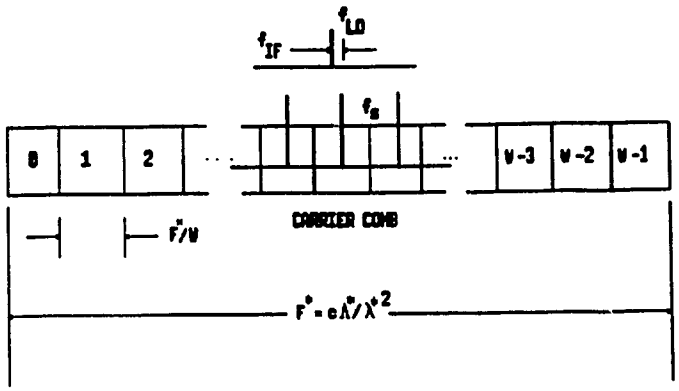

Figure 2.23 FDM Band.

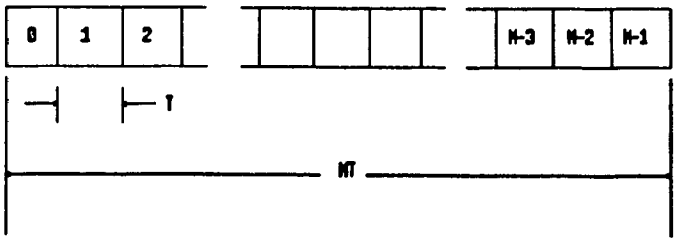

Figure 2.24 TDM Band.

2.2.2 Code Division Multiplexing

In code division multiplexing CDM, each bit is sub-divided into a number of "chips" consisting of 1s and 0s. The chip sequence constitutes a code that permits a bit stream broadcast on a network to be selected by means of a correlation process at the receiver destination. A large number of chip codes can be assigned to different users; however, the number of orthogonal codes that can be used simultaneously on the network is substantially less than the number of chips so that, perhaps, less than a quarter as many channels are available as for a TDM system with equivalent network bandwidth.

2.3 Detection Methods

The challenge of photonic research today is to exploit the large bandwidth offered by the single mode fibers by using FDM or WDM. Various detection schemes are available. Among these we mention the Wavelength or Frequency Division Multiplexing (WDM/FDM) with direct detection, and coherent (heterodyne or homodyne) detection.

2.3.1 Principle of Direct Detection

Direct detection of light pulses implies a photo detection that converts light energy into electrical signals. The detection mechanism is based upon photon counting. In the case of binary transmission, a *one* or *zero* is translated into the presence or absence of optical energy. This mechanism is illustrated in Figure 2.25. This single pulse description can be extended to an entire data wave by assuming that superposition holds for optic fiber transmission. When an Avalanche detector is used to gain optical amplification, fluctuations get larger as the average value gets large; consequently, losses cannot be neglected. Thus, one of the chief motivations for turning to coherent techniques is to minimize this loss in detector sensitivity [28]. For FDM with direct detection, we may consider a simpler scheme for demultiplexing the channels. We can use a narrowband

transmission filter to reject the unwanted channels and employ a direct detection receiver as shown in Figure 2.26.

2.3.2 Principle of Coherent Detection

Figure 2.27 shows the principle of coherent detection. The optical process is similar to radio mixing using an average power detector, a weak signal is first combined using a partially silvered mirror or an optical fiber coupler with a locally generated wave or Local Oscillator (LO) signal. The combined wave is then detected using a photo-diode, which can be viewed as an ideal square-law device since its output current is proportional to the optical intensity [17]. The result of this mixing process is a modulation of the average detector detector photo-current at a frequency equal to the difference between the frequencies of the signal, $A_s cos(\omega_s t + \rho_s)$, and the LO, $A_{lo} cos(\omega_{lo} + \rho)$

$$I_{photo} = 1/2\, A_s^2 + 1/2\, A_{lo}^2 + A_s A_{lo} cos[(\omega_s - \omega_{lo})t + (\rho_s - \rho_{lo})]. \qquad (2.11)$$

The new electronic signal is called the Intermediate Frequency (IF) signal. When the signal and LO frequencies are identical, the process is called homodyne detection and the information appears directly at baseband frequencies (i.e., near zero frequency), otherwise the process is called heterodyne detection. Figure 2.28 shows the basic elements of heterodyne and homodyne optical receivers. The term *coherent* is used in optical communication literature to refer to any heterodyne or homodyne process.

Since the amplitude of the IF signal is proportional to the product of the input signal and LO amplitudes, the IF power can be made arbitrarily large compared with amplifier noise by increasing the LO power. That means that a weak signal, mixed with a strong local oscillator wave, results in an effective signal gain proportional to the local oscillator amplitude and can be substantial. This optical gain is extremely valuable since it increases the signal strength before the signal reaches the detection stage and becomes subject to the inevitable noise from components after detection [29].

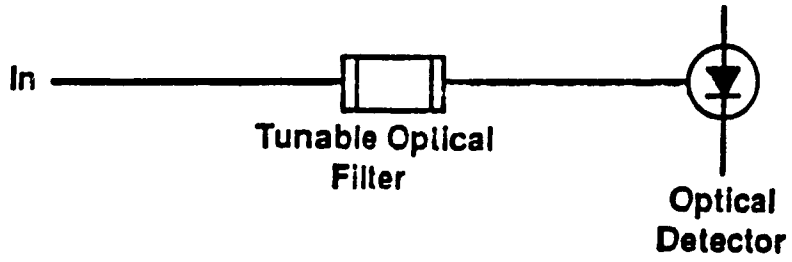

Figure 2.25. Direct Detection.

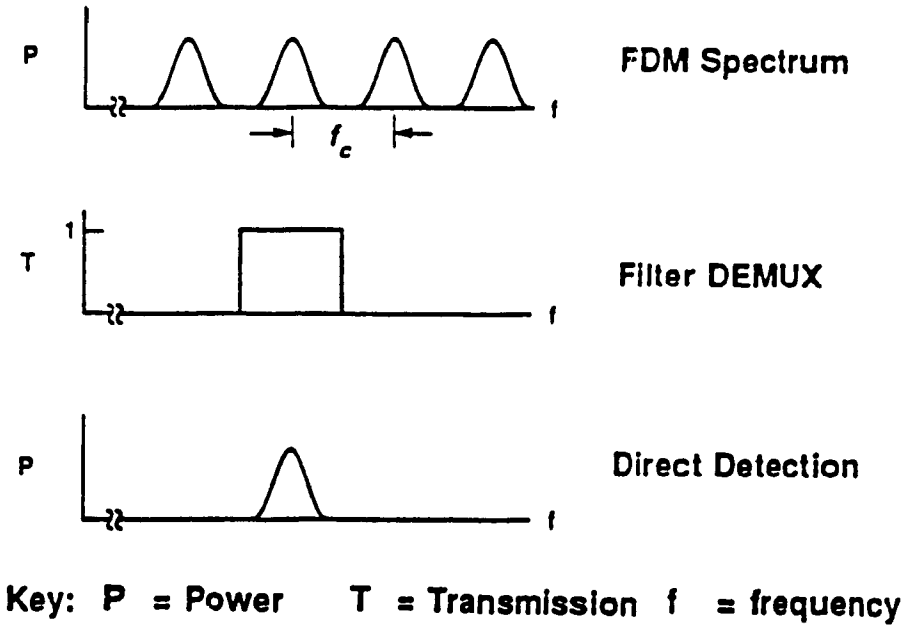

Figure 2.26. Non-Coherent DEMUX and Detection.

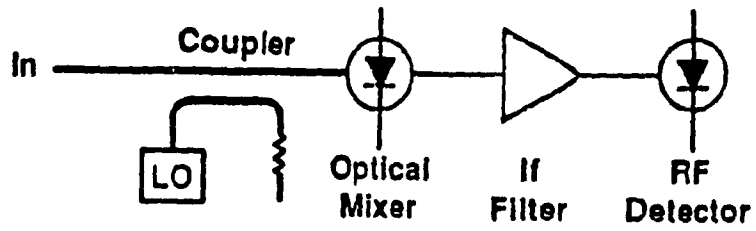

Figure 2.27. Coherent Detection.

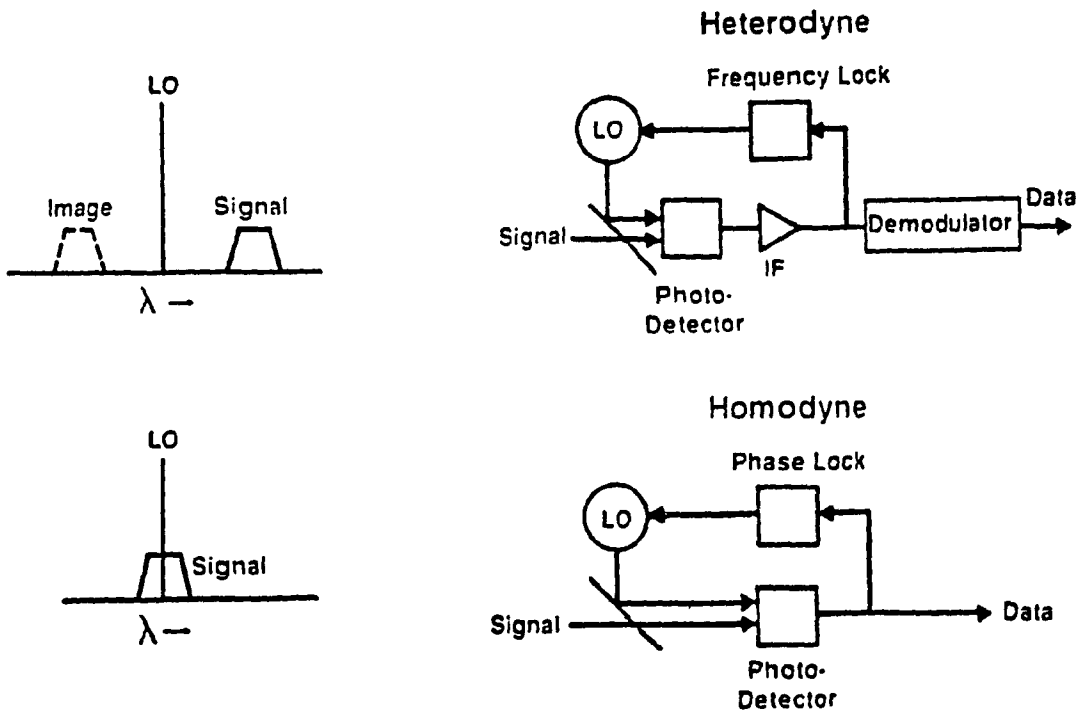

Figure 2.28. Coherent Receivers.

Compared to direct-detection receivers, the heterodyne receivers are about 10 dB more sensitive but require the added cost and complexity of high-power, optical LO, as well as polarization diversity or control of the signal to assure efficient mixing with the LO.

A coherent FDM network is shown in Figure 2.29. Each terminal is provided both an input and an output fiber connected to the centrally located coupler. By analogy to the present telephone system, one can assign fixed wavelengths to the receivers and provide tunable lasers to the transmitters, thereby making it possible for any transmitter to access any receiver by tuning to its assigned frequency (i.e., "phone number"). Alternately, it may be desirable to fix the transmitter wavelengths and provide tunable receiver LOs to allow for the additional possibility of a broadcast mode in which many receivers simultaneously detect the same channel.

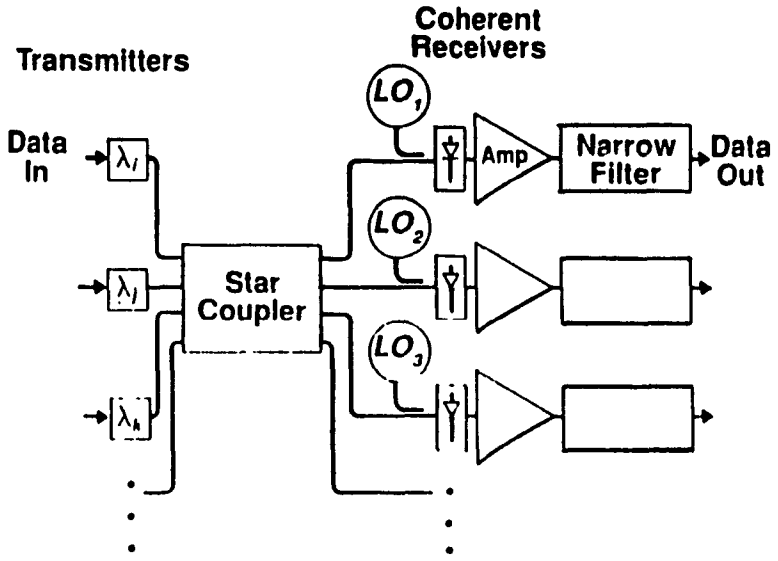

Figure 2.29. FDM Coherent Star Network.

CHAPTER THREE

PERFECT SHUFFLENET

Optical fiber is primary a point-to-point medium. This is how it has been used in Wide Area Networks (WANs). The optical fiber is now introduced to multiuser Local and Metropolitan Area Networks where many users share the transmission capabilities of the optical fiber. In this chapter, a new local network architecture, ShuffleNet, is presented which appears particularly well-suited for using the optical fiber as a transmission medium, and to share this transmission medium among many users by using time , frequency or wavelength multiplexing. As we will see, a number of physical configurations may be employed to implement ShuffleNet.

3.1 The General Perfect Shuffle

In this section, we introduce the ShuffleNet connectivity graph in which stations are arranged in k columns, each consisting of P^k stations. Each of the P^k stations in a column has P arcs directed to P different stations in the next column. If the stations in a column are numbered from 0 to P^k-1, station j has arcs directed to stations i, i+1, ..., and i+P-1 in the adjacent column; where i = (j mod P^{k-1}) P. There are a total of P^{k+1} directed arcs to connect 2 successive columns. All the columns are arranged in a fixed shuffle pattern, with the last column connected to the first to form a cylindrical pattern. The total number of stations is given by

$$N = kP^k \quad ;k = 1,2,.... \quad P = 1,2,..... \tag{3.1}$$

Figure 3.1 shows the connectivity of an 18-station (P=3, k=2) ShuffleNet, where the first column is repeated on the right to show the cylindrical nature of the connectivity graph.

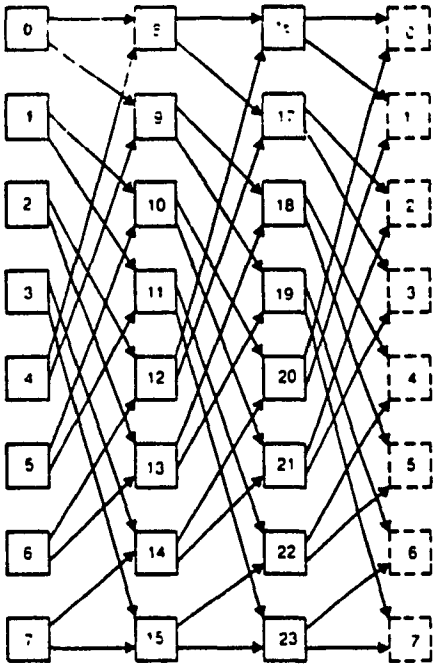

Figure 3.1. An 18-station (P=3, k=2) ShuffleNet.

The total number of links in the ShuffleNet is equal to k times the number required to connect two consecutive columns.

$$L=kP^{k+1}=PN \tag{3.2}$$

In our study, we are interested in configurations suitable for Metropolitan Area Networks (MAN) where there are approximately 10000 stations. There are a number of different values of k and P which may be used as shown in Table 3.1. The case of P = 1 corresponds to the connectivity achieved in a ring network, and the case of k = 1 corresponds to the connectivity achieved with a single-channel broadcast bus [3]. As a result of this, the ShuffleNet topology is general in that it may assume one of a large range of forms, a ring to a bus by the control of a single parameter, the connectivity between stations, and offers the possibility of adaptivity with load.

Table 3.1 The Total Number of Stations as Function of P and k

P	k	N
1	10000	10000
2	10	10240
3	7	15309
5	5	15625
7	4	9604
8	4	16384
15	3	10125
17	3	14738
10000	1	10000

Let h be the number of hops, and $n(h)$ be the number of stations h hops from the source.

For P>1 then

$$n(h)=\begin{cases} P^h & ;1\le h\le k-1 \\ P^k-P^{(h-k)} & ;k\le h\le 2k-1 \end{cases} \tag{3.3}$$

and for P=1

$$n(h)=1 \qquad ;h=1,2,.....,k-1 \tag{3.4}$$

Hence the expected number of hops between two randomly selected stations is given by [3]

$$\overline{H}=E[hops]=\frac{kP^k(P-1)(3k-1)-2k(P^k-1)}{2(P-1)(kP^k-1)} \tag{3.5}$$

3.2 Physical Configuration

The ShuffleNet configuration describes the logical connectivity between station. There are many physical configurations that can be used for the implementation of a photonic network with large number of stations in the ShuffleNet logical configuration. The configuration considered here can be grouped into two classes: basic and compound, based on the topology of their data networks.

3.2.1 Basic Configuration

There are three basic physical configurations that may be used to implement the logical ShuffleNet, the bus, the tree and the star.

3.2.1.1 Bus Configuration

The first basic configuration we consider is the bus configuration. This configuration differs from other configurations by the fact that the network is based on a linear bus topology as shown in Figure 3.2. Each station's traffic is first injected into the "talk side" of the bus, via directional couplers, then broadcast to the receivers on the "listen side", via a second set of couplers. The Distributed Queuing Dual Bus (DQDB) uses logical buses for the media access and interconnection of nodes via point-to-point optical links [32]. Although attractive for use with coaxial cable, this architecture

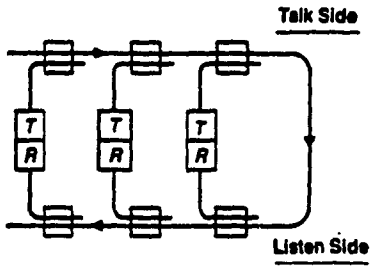

Figure 3.2. Linear Bus Configuration.

is impractical with fiber because it wastes signal power: In an N-station network only P/N^2 useful power is delivered to each receiver (compared to P/N for the star). The poor power efficiently of the bus topology stems from losses associated with coupling power into the "talk side" from the individual transmitters. However, amplifiers could be used to ameliorate this difficulty, and the bus becomes more viable, where the same power efficiency as the star can be obtained [22].

3.2.1.2 Tree Configuration

The second basic configuration we consider here is the tree configuration shown in Figure 3.3. This configuration differs from the star configuration by the fact that the network is based in a minimum-depth binary-tree topology to minimize the number of couplers between transmitter and receivers. The tree configuration requires that the number of stations in the network be a power of 2. Furthermore, in order to uniquely determine the tree when the number of stations N is not a power of 2, we require that the following procedure be used.

We consider the stations in the network to be indexed from 1 to N, and denote the transmitter of the station i by T_i (see Figure 3.3). We let A denote the funneling point of the entire network, and we consider A to be located at the top position of the tree. Then, we divide the transmitters, as evenly as possible, into two groups; the first group consists of transmitters T_0 to $T_{\lfloor N/2 \rfloor}$, and the second group consist of transmitters $T_{\lfloor N/2 \rfloor+1}$, to T_N. $\lfloor x \rfloor$ denotes the largest integer not greater than x. Now we connect the first group and the second group to the point A_0 and A_1 respectively as shown in Figure 3.4. Then we connect the points A_0 and A_1 to funneling point A. Finally, each one of the two groups will represent a minimum-depth-tree configuration which is constructed according to the recursive procedure described here, with A_0 and A_1 as the funneling points for the left and right subtrees respectively.

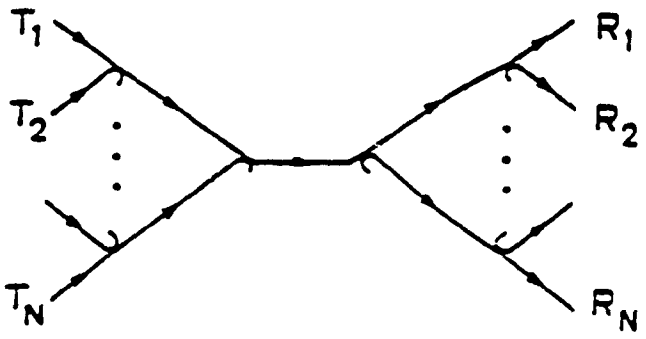

Figure 3.3. Tree Configuration.

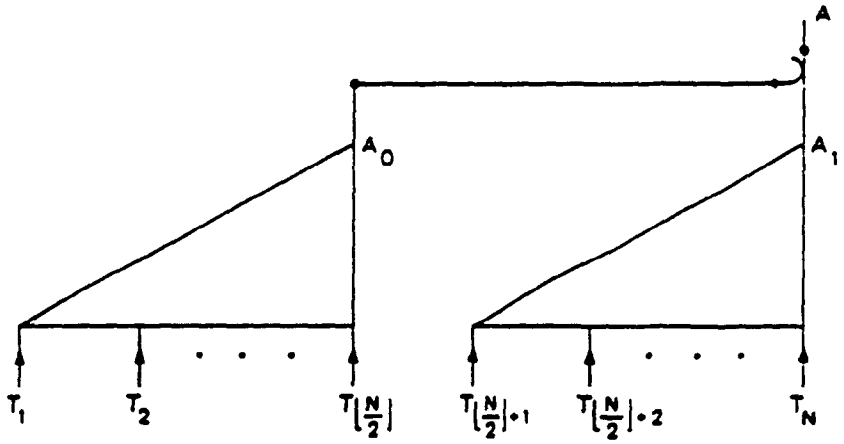

Figure 3.4. Construction of the Minimum-Depth Binary-Tree.

An important figure of merit of a fiber-optic LAN architecture with passive taps is the maximum number of stations that can be connected to it. It is well known that light detectors use much more signal power than their electronic counterparts (there is no much thing as a high impedance light sensor). Thus, the number of passive taps that can be cascaded on a linear bus or on a tree path is fairly limited. As we shall see, the tree structure offers substantial advantages over the linear bus in this regard. Still even in the tree, the total number of stations is fairly modest unless intermediate amplification is used. Here again, the tree permits more cost-effective amplification strategies than the bus.

To determine the maximum number of stations that can be supported, we must require that the signal transmitted by the light source (laser or LED) be properly detected at the end of the longest network path by the light detector. First some definitions and assumptions are in order. Let M^* be the power margin (in dB), M^* is defined as

$$M^* = 10\log_{10}(P_T / P_R) \tag{3.8}$$

where P_T is the available optical transmitter power and P_R is the minimum receiver power that provides a tolerable bit-error rate (BER). Typically, M^* is on the order of 40 dB. The power reduction at each level due to the tree coupler is assumed to be 4 dB (3 dB for power splitting, and 1 dB for connector excess loss; a fairly conservative estimate). We also assume another reduction of 3 dB at the receiver of each station (2 dB for power spilling, and 1 dB for excess loss). The total number of stations in the network is given by

$$N = 2^L \tag{3.7}$$

where L the number of levels in the tree (see Figure 3.5). If no intermediate amplification is provided, and if the same assumptions mentioned above hold for the transmitting side and the receiving side, this case corresponds to a particular case of the general case mentioned by Gerla [7], in which several stations in a bus configuration are connected to a

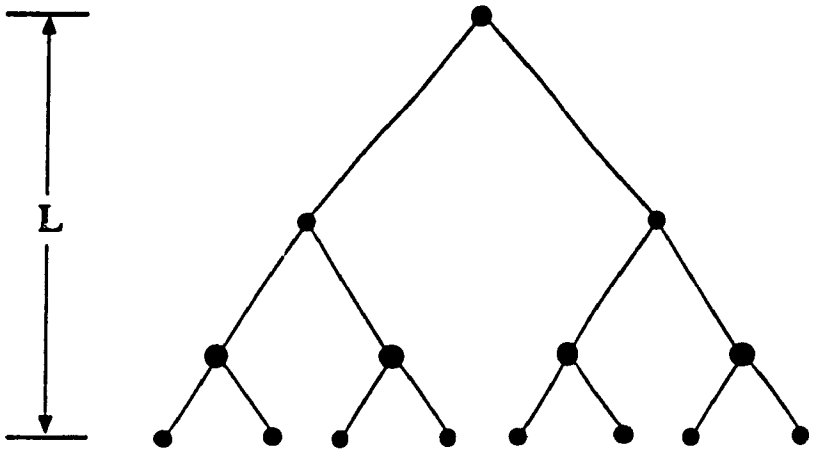

Figure 3.5. Binary Tree.

tree. In our particular case, we connect only one station at the end of each branch of the tree, this gives us the following inequalities.

For the general case, where C is equal to the number of stations in the bus we have

$$2(4L+3) \leq M^* \tag{3.8}$$

For the special case (C=1)

$$N \leq N(\frac{M^*}{6} - \frac{4L}{3}). \tag{3.9}$$

Noting that the total number of stations N is given by equation (3.7), if we substitute equation (3.7) into equation (3.9), we will have

$$N \leq 2^L(\frac{M^*}{6} - \frac{4L}{3}). \tag{3.10}$$

For the case of M^* =40, equation (3.10) becomes

$$N \leq 2^L(6.66 - 1.33L). \tag{3.11}$$

the maximum number of tree levels correspond to the case of

$$L \leq 5.66/1.33 \tag{3.12}$$

this relation will give us L = 4. From equation (3.11), the number of stations is function of the number of tree levels. We note that the maximum N = 16 is obtained with L = 4. For L = 0, i.e. single bus structure, the maximum is N = 6. Thus the tree structure improves the situation (from 6 to 16), although the maximum number of supported stations is still too low for metropolitan area applications.

Station connectivity can be greatly improved by introducing an amplification stage at the root of the tree to amplify the signal that has been degraded at the transmitting side. In this case, we deal only with the receiving side. Then, the following inequality [7] must be satisfied:

$$4L+3 \leq M^{*}. \tag{3.13}$$

or

$$N \leq N(\frac{M^{*}}{3} - \frac{4L}{3}) \tag{3.14}$$

we have by substituting equation (3.7) into equation (3.14), and taking $M^{*} = 40$ we will have

$$N \leq 2^{L}(13.33 - 1.33L). \tag{3.15}$$

The maximum number of stations for this case is obtained for L = 9, and it is equal to 512. The comparison to the previous result shows that amplification is much more effective in terms of increasing the maximum number of stations.

3.2.1.3 Star Topology

The first basic configuration to implement a photonic network is the star topology. In this configuration we use an NxN star coupler (where N is the number of stations), and a set of fibers through which the transmitters and receivers are connected to the star coupler as shown in Figure 3.6. There are two kinds of star coupler that can be used in a photonic network:

- The active star, in which all incoming optical signals are converted to electrical and then converted back to optical for outgoing signals. Each message can be broadcast to all stations from the central node with appropriate address headers.
- A passive star has similar topology properties but no active processing or regeneration takes place at the node; an incoming signal from a given station is broadcast to all N stations of the network.

For the following part we concentrate our study on the passive star which is less complicated and faster than the active star [1].

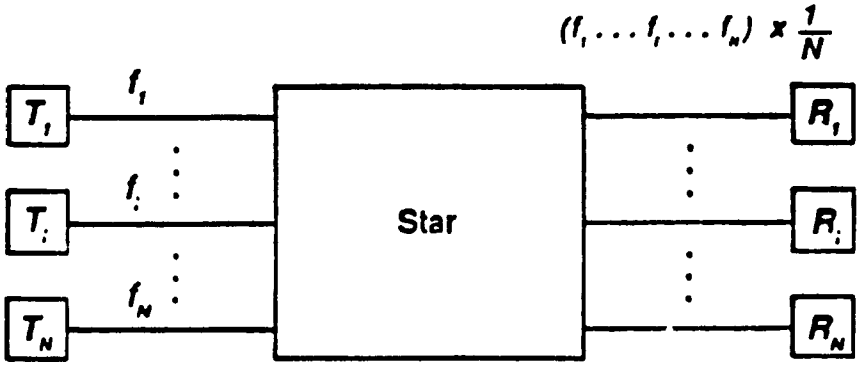

Figure 3.6. Passive Star Coupler.

A single-mode-fiber passive star coupler is a key component in many architectures of high speed optical-area networks (LAN's). In the ideal case, for an NxN star coupler, all N input and N output ports are equivalent. Then, for any given station i that transmit a total power $P_T(i)$, this power is divided equally among all the N output ports. Then $P_T(i)/N$ will appear at each of the output ports (and none at the input ports), including port i. In practice, of course the power division may not be equal and the output distribution may vary with the input port. In addition, there will be some excess power loss due to absorption and scattering, this is not considered in Figure 3.6. For an excess power loss, ΔP, we have [1]

$$\frac{\Delta P(i)}{P_T(i)} = 1 - \frac{\sum_{j=1}^{N} P_R(j,i)}{P_T(i)}$$

$$\approx 1 - \beta; \tag{3.16}$$

where $P_R(j,i)$ is the power received at j due to $P_T(i)$. For simplicity we may assume that the star coupler uniformly distributes the input signals across its output ports and define a constant β such that

$$\frac{P_R(j,i)}{P_T(i)} \approx \beta/N \tag{3.17}$$

for all j and i with (1-β) the excess loss factor, and 10 $\log_{10}\beta$ the excess loss in dB.

To create a broadcast-type LAN, where a message can be transmitted and received simultaneous by most or all the stations, the NxN star can serve as the central node in a N-stations LAN, where each station would be connected by two fibers, one for transmission to the input side of the star, and the other for reception from the output side of the star. We attempt to apply any of a number of protocols such as wavelength-division

multiple access (WDMA) and time-division multiple access (TDMA), to this structure.

Finally, the main advantage of the star architecture over other LAN architectures such as the bus, where the various stations are coupled in succession to a single fiber, is its small excess loss. For example the excess loss for an N-station star increases only logarithmically with N as shown in the previous paragraph, while that of an N-station bus increases linearly with N [4]. The difference in loss can be quite significant, especially for large values of N, which is the case in our problem.

3.2.2 Compound Configurations

The basic configurations which are described in the previous section have some limitation on the total number of stations in the network. The technique of interconnecting several trees with a passive modular star, as shown in figure 3.7 is an effective way of improving the total number of stations. Recall that the number of stages in a modular star is $\log_2 S$ where S is the number of ports[4]. Each stage introduces a 4 dB attenuation. Using the assumptions in the previous section, a system with a four-stage star (S=16) and with a three-level tree can support 8.16 = 128 stations without requiring any amplification. This is a major improvement with respect to the 16 stations in a tree. If amplification is used, the modular star permits a dramatic increase in the total number of stations. Assuming that amplifiers are used at the inputs and the outputs of the star, a configuration with a 10-stage star (1024 inputs and outputs) or the equivalent star that uses the Free-Space planar guide, and a 3-level tree becomes feasible (from the power budget standpoint). This configuration supports up to 16384 stations. This number is large enough to support our network which is designed to accommodate up to 10000 stations

3.3 Network Architecture Overview

One of the novel properties of the physical topologies described in the previous

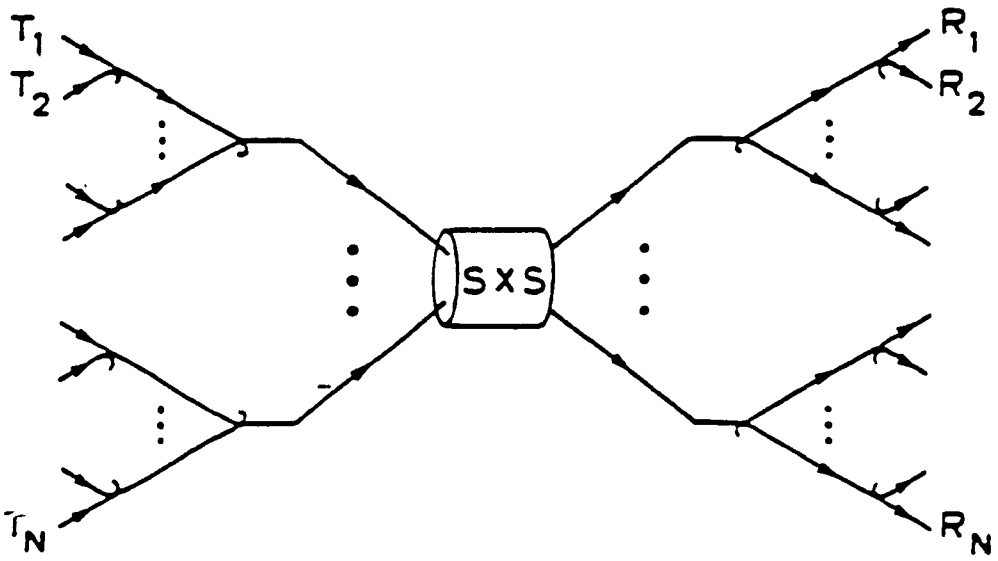

Figure 3.7. The Tree-Star-Tree Configuration.

section is that we can map any logical topology onto a given physical topology. This property, which is illustrated in Figure 3.8, shows how a ShuffleNet with eight stations (Figure 3.9) is mapped onto a tree topology for the distribution of optical signals. There are 16 WDM channels in use, and each station has two transceivers, the tuning of which is represented by the dotted arcs in Figure 3.8, which depicts only the logical connectivity between stations without regard for their embedding in the plane or the manner in which they are physically connected. Each station has two optical transmitters, two optical receivers, and one electronic user port. The 16 WDM channels are labeled $\lambda_0 - \lambda_{15}$. A packet arrives at the station through the incoming user port or one of the receivers, it is buffered in fast memory, its header is examined, and the station makes a quick routing decision to send the packet through a specific transmitter or the outgoing user port. We assume that each station has ample packet-buffer space, which effectively eliminates the chance of buffer overflow, except in overload situations. The idea of relaying messages from one station to another over different bands is borrowed from radio relay networks [3]. This network uses multihopping as the method of delivering a message from a sender to a receiver. In Figure 3.9 for example, station 3 could send a message to station 4 via the path $3 \rightarrow 6 \rightarrow 0 \rightarrow 4$. The routing decision at each station is based on address information contained in an arriving packet's header, possibly using self-routing switching techniques to minimize source-to-destination delays [10]. Figure 3.10 shows a block diagram of a station network with two transmitters, two receiver, a 3x3 switch for routing packets to their appropriate output ports, and buffers for queuing multiple packets destined for the same port.

Examing the example of Figure 3.9, we notice that every WDM channel has precisely one transmitter and one receiver. An alternative to such a dedicated channel ShuffleNet is the shared channel where several stations can access a WDM channel. There are several potential motivations for the use of shared channels in our network,

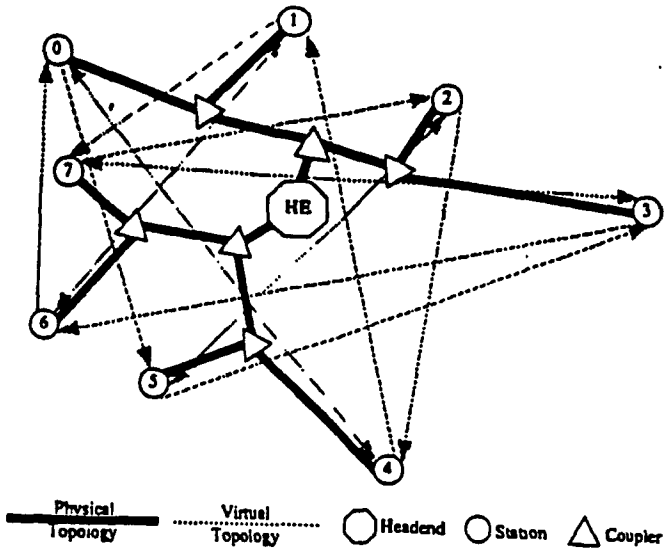

Figure 3.8. An 8-station ShuffleNet Implemented as a Physical Tree.

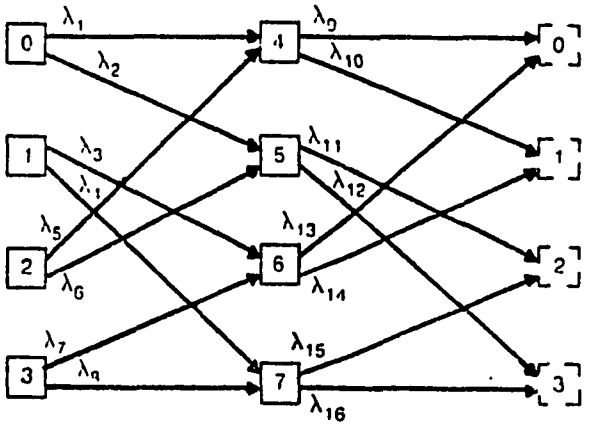

Figure 3.9. An 8-station ShuffleNet Connectivity Graph.

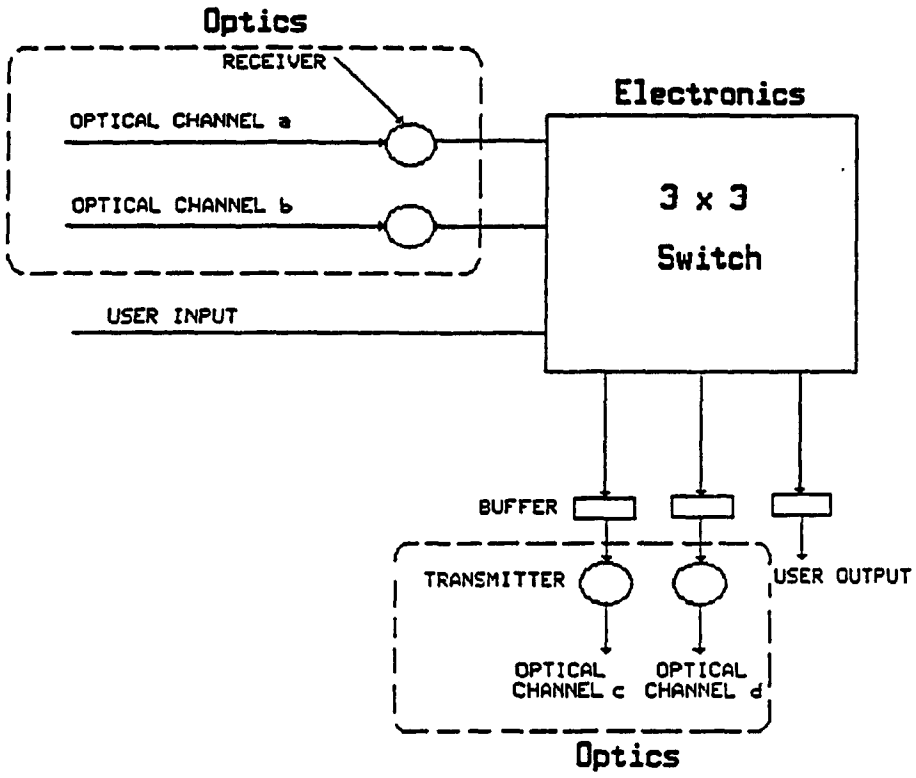

Figure 3.10. Block Diagram of a Network Interface.

including the possibility of using fewer WDM channels, and reducing the number of transmitters.

If we assume that the traffic is Time Division Multiplexing (TDM), a parameter which is called the multiplexing factor M specifies the number of (TDM) channels that share a single wavelength. Let T_r be number of transmitters and R_e the number of receivers in each of the stations; clearly $1 \leq T_r \leq P$, and $1 \leq R_e \leq P$. W is the total number of wavelengths that are available, or that can be fabricated on one fiber. The number of channels available is equal to

$$T_c = MW \tag{3.18}$$

In order for the system to work the number of physical channels should be greater than or equal to the number of logical channels. Then the relationship among W, M, and L (the total number of links) is

$$MW \geq PN \tag{3.19}$$

Then, M will be equal to

$$M = \left[\frac{PN}{W} \right]^{+} \tag{3.20}$$

$[]^{+}$:smallest integer greater than.

CHAPTER FOUR

PERFORMANCE CALCULATIONS

SHUFFLENET WITH NO BANDWIDTH RESTRICTIONS

We turn now to consider the performance of the ShuffleNet as measured by delay as a function of throughput. The delay of a message is defined as the time interval between its arrival at the system and its exit from the system. This delay encompasses queuing, transmission, propagation, and processing delay. We shall carry through an analysis of delay under the assumption that circulating traffic has priority over newly generated traffic. We also assume that the traffic is Time Division Multiplexing (TDM) and the message length is equal to the slot duration.

4.1 Presentation of the Node in a ShuffleNet

The model of the node may be as shown in Figure 4.1, where the P input lines enter through a processor that distributes the traffic to output lines. The processor is just a commutator since the traffic is TDM on the output lines. The output line queues are where congestion would occur. The model used for each output line is shown in Figure 4.2. A discrete time statistical multiplexer is used for modeling our output line. Several assumptions are used :

1) Arrivals are governed by a Binomial process.

2) A priority discipline is used.

In this section, we will study multiplexer operation in a two state Markovian environment where the states indicate server availability and nonavailability, respectively. Each state is characterized by its Binomial arrival process.

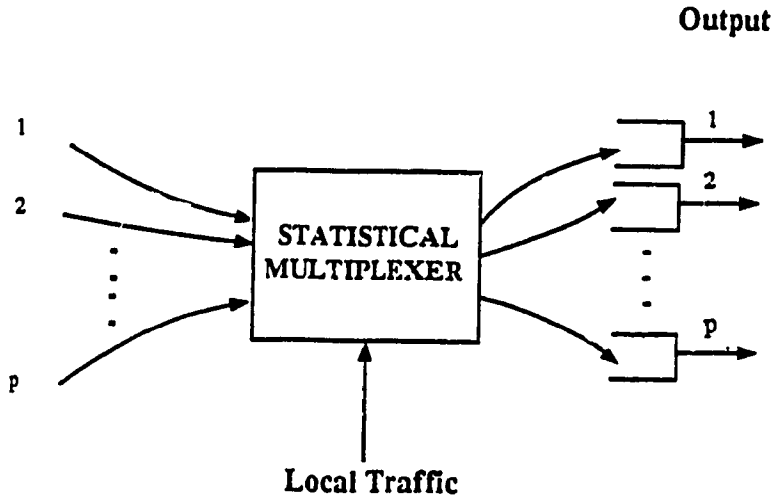

Figure 4.1. The Node Model.

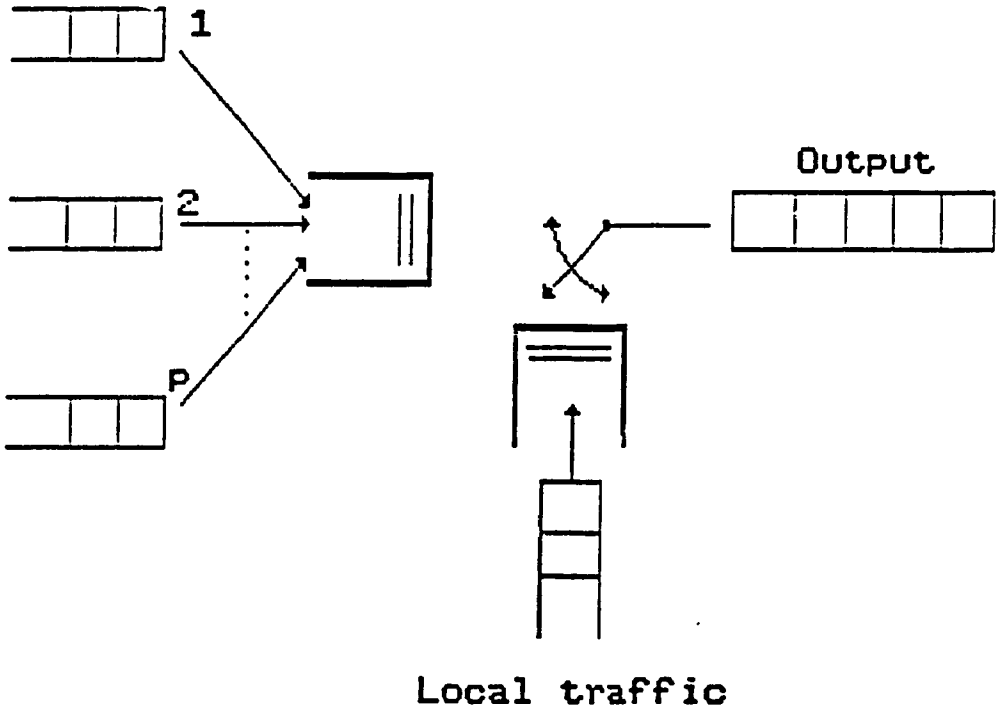

Figure 4.2. The Output Line.

A multiplexer divides time into fixed size intervals called slots. Data arrive into the multiplexer in fixed size units which we shall refer to as packets. Exactly one packet can be transmitted during one slot. The breakdown model can be used analyze a multiplexer with a head of the line fixed priority preemptive queuing discipline. For simplicity assume there are two classes $c=1,2$ of packets with class $c=1$ having the higher priority, and class $c=2$ having the lower priority.

4.2 Traffic Evaluation for the Symmetric Case

The traffic generated by one source can be represented as:

$$\Lambda' = \sum_{h=1}^{2k-1} \lambda(h) n(h) \tag{4.1}$$

where $\lambda(h)$ is the amount of traffic that is destined for each station at distance h and $n(h)$ is the number of stations at distance h. In the the purely symmetric case the amount of traffic destined to all N-1 other stations in the system is the same. Then we will have $\lambda(h)$ is a constant equal to λ, for all h. From Hluchyj and Karol [3], if we assume that $P > 1$, then $n(h)$, the number of stations at distance h, is given by

$$n(h) = \begin{cases} P^h & ;1 \le h \le K-1 \\ P^k - P^{(h-k)} & ;k \le h \le 2k-1 \end{cases} \tag{4.2}$$

and for P=1

$$n(h) = 1 \qquad ;h = 1,2,.....,k-1 \tag{4.3}$$

Now, we wish to calculate the usage of network resources by each source. Clearly, traffic which travels over more hops uses more system bandwidth. If each link traversed uses one unit of bandwidth, the bandwidth used by a source transmitting to a destination h hops distant is $\lambda(h)$. Summing over all such receiving stations and over all hops, the total network bandwidth used by a single source will be equal to:

$$B = \sum_{h=1}^{2k-1} h\lambda(h)n(h) \tag{4.4}$$

In the symmetric case, we have

$$B = \lambda \sum_{h=1}^{2k-1} hn(h)$$

$$= \lambda \sum_{h=1}^{2^k-1} n(h) = \lambda(N-1) = \lambda(kP^k-1)$$

$$= \lambda \sum_{h=1}^{k-1} hP^h + \lambda \sum_{h=k}^{2k-1} h(P^k - P^{(h-k)}) \tag{4.5}$$

Let $l = h-k$ so $h = l+k$

$$B = \lambda \sum_{h=1}^{k-1} hP^h + \lambda \sum_{l=0}^{k-1} (l+k)(P^k - P^l)$$

$$= \lambda \sum_{l=0}^{k-1} lP^k + \lambda \sum_{l=0}^{k-1} kP^k - \lambda \sum_{l=0}^{k-1} kP^l$$

$$= \lambda P^k \frac{k(k-1)}{2} + \lambda k^2 P^k - \lambda k \frac{P^k-1}{P-1}$$

$$= \frac{\lambda[P^k(k^2-k)(P-1)+2k^2P^k(P-1) - 2k(P^k-1)]}{2(P-1)}$$

$$= \frac{\lambda[P^k(P-1)k(3k-1) - 2k(P^k-1)]}{2(P-1)} \tag{4.6}$$

Notice that in the symmetric case E[hops] = $\overline{H}$ is equal to:

$$\overline{H} = \frac{B}{\lambda(kP^k-1)} \tag{4.7}$$

The total bandwidth used by all sources is kP^kB bits/sec.

Now there are a total of kP^{k+1} links in the network. Since the traffic pattern is symmetric each link must carry

$$\Lambda = \frac{kP^kB}{kP^{k+1}} = \frac{B}{P} \quad messages/sec.$$

$$= \frac{\lambda[P^k(P-1)k(3k-1)-2k(P^k-1)]}{2P(P-1)}$$

$$= \frac{\lambda[N(P-1)(3k-1)-2(N-k)]}{2P(P-1)} \tag{4.8}$$

Notice that, if N and λ are held constant, the total traffic on a link is approximately inversely proportional to the connectivity, P. This is the total amount of traffic on each link in the symmetric case. Of this Λ'/P is newly generated. If we go by the usual priority the locally generated traffic $\lambda(N-1)$ is split P ways for each output trunk so:

$$\lambda_{local} = \frac{\lambda(kP^k-1)}{P} = \frac{\lambda(N-1)}{P} \tag{4.9}$$

And the through traffic on a line is:

$$\Lambda_T = \Lambda - \lambda_{local} \tag{4.10}$$

4.3 Queuing Delay

In this section, we derive the average queue length for the first class packets and second class packets, and by using Little's Formula we can find the average delay for each class of packets.

4.3.1 Higher Priority Delay

A priority discipline is used in modeling our communication system, where 2 types

of traffic contend for an output line. Because of the priority discipline the class with lower priority has no effect on the first class [9]. If there is a class one message in the buffer at a slot interval, it is transmitted. Then the calculation of the higher priority delay is reduced to the calculation of the delay over a buffer with P inputs which are multiplexed in the same line. We assume that M TDM channels share the same wavelength. In this case, a link has a single slot which carries a single data unit in a frame.

The queueing model is as shown in Figure 4.3. Through traffic from P incoming links has priority over locally generated traffic. The expected queue length is found to be [9]:

$$\bar{n}_D = \frac{(1-\rho)A'(1,T_F)}{1-A'(1,T_F)} + \frac{A''(1,T_F)}{2[1-A'(1,T_F)]} \tag{4.11}$$

Where

$$A'(1,T_F) = dA(z,T_F)/dz \mid_{z=1} \tag{4.12}$$

$$A''(1,T_F) = d^2A(z,T_F)/dz^2 \mid_{z=1} \tag{4.13}$$

and ρ is the system load and is given by:

$$\rho = \lambda_1 T_F \bar{m} \tag{4.14}$$

where $\bar{m}$ is the average number of data units in a message, λ_1 is the aggregate arrival process to the multiplexer from all sources, and T_F is the frame duration.

Let us assume that $G_{(c)}(z)$ is the generating function for the distribution of the number of class c packets arriving in a frame, $c = 1,2$. Then $A(z,T_F) = G_{(1)}(z)$, and given that each slot contains exactly one message , $\bar{m} = 1$ and equation (4.11) becomes:

$$\bar{n}_D = \frac{(1-\rho)G_{(1)}'(1)}{1-G_{(1)}'(1)} + \frac{G_{(1)}''(1)}{2(1-G_{(1)}'(1))} \tag{4.15}$$

Finally the average delay is given by [9]

$$D_1 = T_F[\bar{n}_D - \rho] + \frac{\rho T_F}{2}$$

$$= \frac{(1-\rho)G_{(1)}'(1)}{(1-G_{(1)}'(1))} + \frac{G_{(1)}''(1)}{2(1-G_{(1)}'(1))} - \frac{\rho T_F}{2} \qquad (4.16)$$

4.3.1.1 The Higher Priority Generating Function

First, the multiplexing on the output line is shown in Figure 4.3. The through traffic looks as it comes from P inputs, with each input generating Λ_T/P messages/sec.

The arrival process for the high priority traffic should be P-Bernoulli processes. The generating function for the high priority traffic will have a binomial distribution, and it is given by

$$G_{(1)}(z) = (1-q+qz)^P \qquad (4.17)$$

Where

$q = \frac{\Lambda_T . T_F}{P}$: is the probability the probability of a message being generated in a frame.

Notice that the average message arrival rate in a frame is $qP = \Lambda_T . T_F$, as it should be.

The first and second derivatives of $G_{(1)}(z)$ at z=1 are equal to

$$G_{(1)}'(1) = +Pq = P\Lambda_T . T/P = \Lambda_T . T_F$$

$$= P\Lambda T - \lambda(N-1)T_F \qquad (4.18)$$

$$G_{(1)}''(1) = (Pq)^2 - Pq^2 = (\Lambda_T . T_F)^2 - \Lambda_T^2 . T_F^2/P$$

$$= (\Lambda^2 - \frac{2\lambda(N-1)\Lambda}{P} + \frac{(\lambda(N-1))^2}{P^2}) T_F^2 (P^2 - P)$$

$$= (PT_F\Lambda)^2 + \Lambda T_F^2[2(1-P)\lambda(N-1) - \Lambda^2] + (1-\frac{1}{P})(\lambda(N-1)T_F)^2 \qquad (4.19)$$

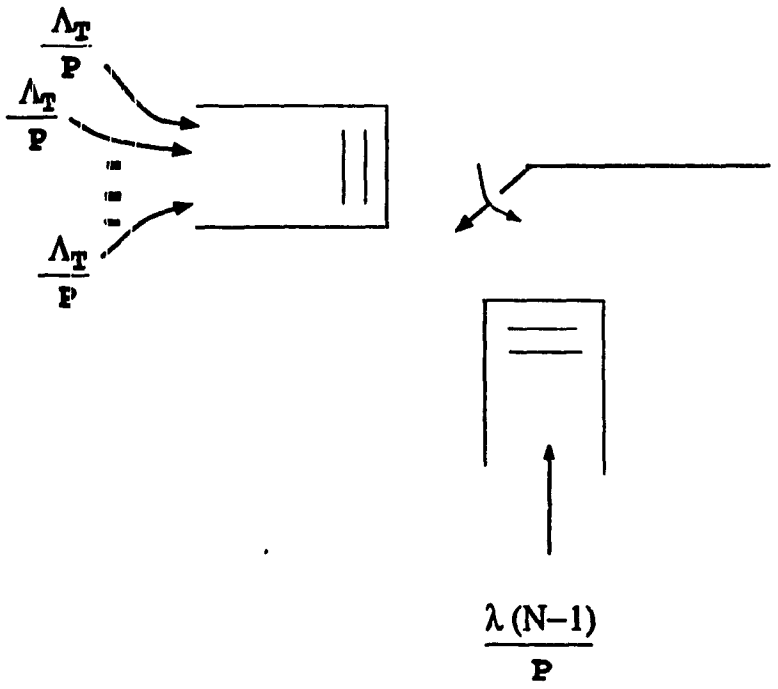

Figure 4.3. The Multiplexing on the Output Line.

4.3.2 Lower Priority Delay

Now we focus our study on the lower priority packets. The low priority packets see a system that periodically breaks down (the breakdown is due to servicing of high priority packets). The time between breakdown periods corresponds to the busy period for the low priority packets because during this period there are no high priority packets and the system can serve the low priority packets. The duration of the breakdown period corresponds to the busy period for the high priority packets because during this period the system is interrupted to serve high priority packets.

Let us assume that $G_{(c)}(z)$ is the generating function for the distribution of the number of class c packets arriving in a frame, $c=1,2$. The expected queue length of the low priority packets $E[L]$ as a function of $G_{(1)}(z)$ and $G_{(2)}(z)$ is given by Towsley [8]. All calculation are shown in Appendix A.

The expression is found to be given by

$$E[L]=G_{(2)}'(1)[1-G_{(1)}'(1)]+\frac{G_{(2)}''(1)+4G_{(2)}'(1)[G_{(1)}'(1)]^2}{2[1-G_{(1)}'(1)-G_{(2)}'(1)]}$$

$$+\frac{G_{(1)}''(1)G_{(2)}'(1)}{2[1-G_{(1)}'(1)][1-G_{(1)}'(1)-G_{(2)}'(1)]} \tag{4.20}$$

Given that λ_2 is the average arrival rate of the class 2 messages, the average delay for the second class messages is given by [9]

$$D_2=T_F(E[L]-\rho_2)+\frac{\rho_2 T_F}{2}$$

$$=G_{(2)}'(1)[1-G_{(1)}'(1)]+\frac{G_{(2)}''(1)+4G_{(2)}'(1)[G_{(1)}'(1)]^2}{2[1-G_{(1)}'(1)-G_{(2)}'(1)]}$$

$$+\frac{G_{(1)}''(1)G_{(2)}'(1)}{2[1-G_{(1)}'(1)][1-G_{(1)}'(1)-G_{(2)}'(1)]}-\frac{\rho_2 T_F}{2} \tag{4.21}$$

4.3.2.1 The Lower Priority Generating Function

For the low priority traffic we assumed to that we have Poisson arrivals, the probability of having i arrivals is equal to

$$p(i\ arrivals) = e^{-\lambda_{local} T_F} (\lambda_{local} T_F)^i / i! \tag{4.22}$$

Where

$\lambda_{local} = \dfrac{\lambda(N-1)}{P}$: is the locally generated traffic, and T_F is the frame duration.

The generating function for the low priority traffic is given by

$$G_{(2)}(z) = e^{-\frac{\lambda(N-1)}{P} T_F (1-z)} \tag{4.23}$$

The first and second derivative of $G_{(2)}(z)$ at z=1 are equal to

$$G_{(2)}'(1) = \frac{\lambda(N-1)}{P} T_F \tag{4.24}$$

$$G_{(2)}''(1) = \left(\frac{\lambda(N-1)}{P} T_F\right)^2 \tag{4.25}$$

4.4 Multiplexing and Processing Delay

4.4.1 Multiplexing Delay

We assume that the traffic is Time Division Multiplexing (TDM). This due to an important parameter, which is called the multiplexing factor M, that specifies the number of (TDM) channels that share a single wavelength. Let T_r be number of transmitters and R_e the number of receivers in each of the stations; clearly $1 \le T_r \le P$, and $1 \le R_e \le P$. W is the total number of wavelengths that are available, or that can be fabricated on one fiber. The number of channels available is equal to

$$T_c = MW \tag{4.26}$$

In order for the system to work, the number of physical channels should be greater than or equal to the number of logical channels. Then the relationship among W, M, and L (the total number of links) is

$$MW \geq PN \tag{4.27}$$

Then, M will be equal to

$$M = \left[\frac{PN}{W}\right]^{+} \tag{4.28}$$

$[]^{+}$:smallest integer greater than.

Finally, the multiplexing delay is given by

$$D_M = \frac{MT}{2} \tag{4.29}$$

This is the average time required for a message to access a slot that has been assigned to it.

4.4.2 Processing and Propagation Delay

Other sources of delay are the processing at each node and the propagation delay over the optical links. Both kinds offer the total delay in the same way, increasing linearly with the number of hops. They are lumped together in a single parameter, D_p.

4.5 Total Delay

The sources of delay are queuing delay, multiplexing delay, and processing delay at the node. For each message we have two kinds of queuing delay as we mentioned before. The first queuing delay encountered by a message is when it enters the system; this is equal to D_2. At each subsequent hop an additional delay component is encountered which is equal to D_1. For each hop we then add the transmission delay T, the

multiplexing delay D_M and the processing delay D_p. The total delay is given by

$$D_T = D_2 + D_1(\bar{H}-1) + (T + D_M + D_p)\bar{H} \tag{4.30}$$

The factor T here is simply the time required to transmit a message in a slot.

4.6 Numerical Results

After finding the expression of the queuing delays D_1 and D_2 as a function of the first and second derivative of $G_{(1)}(z)$ and $G_{(2)}(z)$, then the final expression of D_1 and D_2 is only a matter of substitution. If we substitute equations (4.18) and (4.19) in equation (4.16) where

$$\lambda_1 = \Lambda_T = \Lambda - \frac{\lambda(N-1)}{P} \tag{4.31}$$

and

$$\rho = \Lambda_T T_F = \Lambda T_F - \frac{\lambda(N-1)}{P} T_F. \tag{4.32}$$

Then, the final expression for the high priority delay is given by

$$D_1 = \frac{\Lambda_T T_F}{2} + \frac{(\Lambda_T T_F)^2(1-1/P)}{2(1-\Lambda_T T_F)}$$

$$= [(\Lambda - \frac{\lambda(N-1)}{P})T_F][\frac{1}{2} + \frac{(\Lambda - \frac{\lambda(N-1)}{P})(1-\frac{1}{P})T_F}{2(1-\Lambda+\frac{\lambda(N-1)}{P})}], \tag{4.33}$$

and by substituting equations (4.18), (4.19), (4.24), and (4.25) in equation (4.21) this gives us the final expression for the queuing delay for the lower priority messages where

$$\lambda_2 = \frac{\lambda(N-1)}{P} \quad \text{and} \quad \rho_2 = \frac{\lambda(N-1)T_F}{P}. \tag{4.34}$$

Then

$$D_2=\lambda_2 T_F[1-\Lambda_T T_F]+\frac{(\lambda_2 T_F)^2+4\lambda_2 T_F[(\Lambda_T T_F)^2(1-1/P)]}{2[1-\Lambda T_F]}$$

$$+\frac{\lambda_2 T_F(\Lambda_T T_F)^2(1-1/P)}{2[1-\Lambda_T T_F][1-\Lambda T_F]}-\frac{\lambda_2 T_F}{2} \tag{4.35}$$

4.6.1 Results

For our final results we introduce some numerical values that will be used in our program. C_w is the bit rate per wavelength

$$C_w = 1\ Gbit/sec \tag{4.36}$$

C_L is the capacity per link

$$C_L = \frac{C_w}{M} \tag{4.37}$$

W is the number of wavelengths available

$$W = 1000 \tag{4.38}$$

After writing a program that calculates the total delay, we can obtain different curves which depend on the number N, the configuration used (P, k) which affects $\bar{H}$ and M, and the processing delay which includes the propagation delay. As a first part we try to vary the processing for a given configuration, using 3 different values of $\frac{D_p}{T}$ (.1, 1, 10) for two different configurations (N=10240, k=10, P=2, and N=10125, k=3, P=15). These results are shown in Figure 4.4 and Figure 4.5.

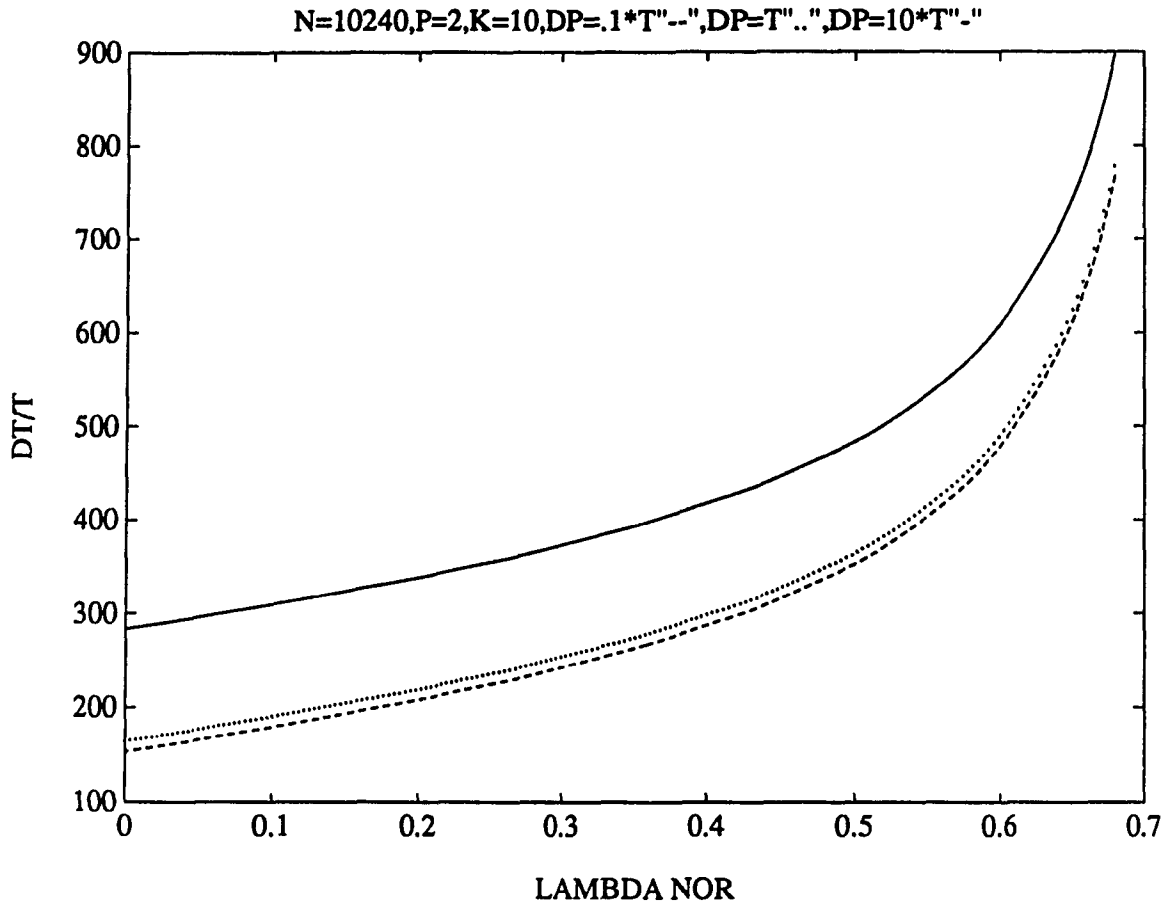

Figure 4.4. Performance Results as Function of D_p for the Case of N=10240, P=2, k=10.

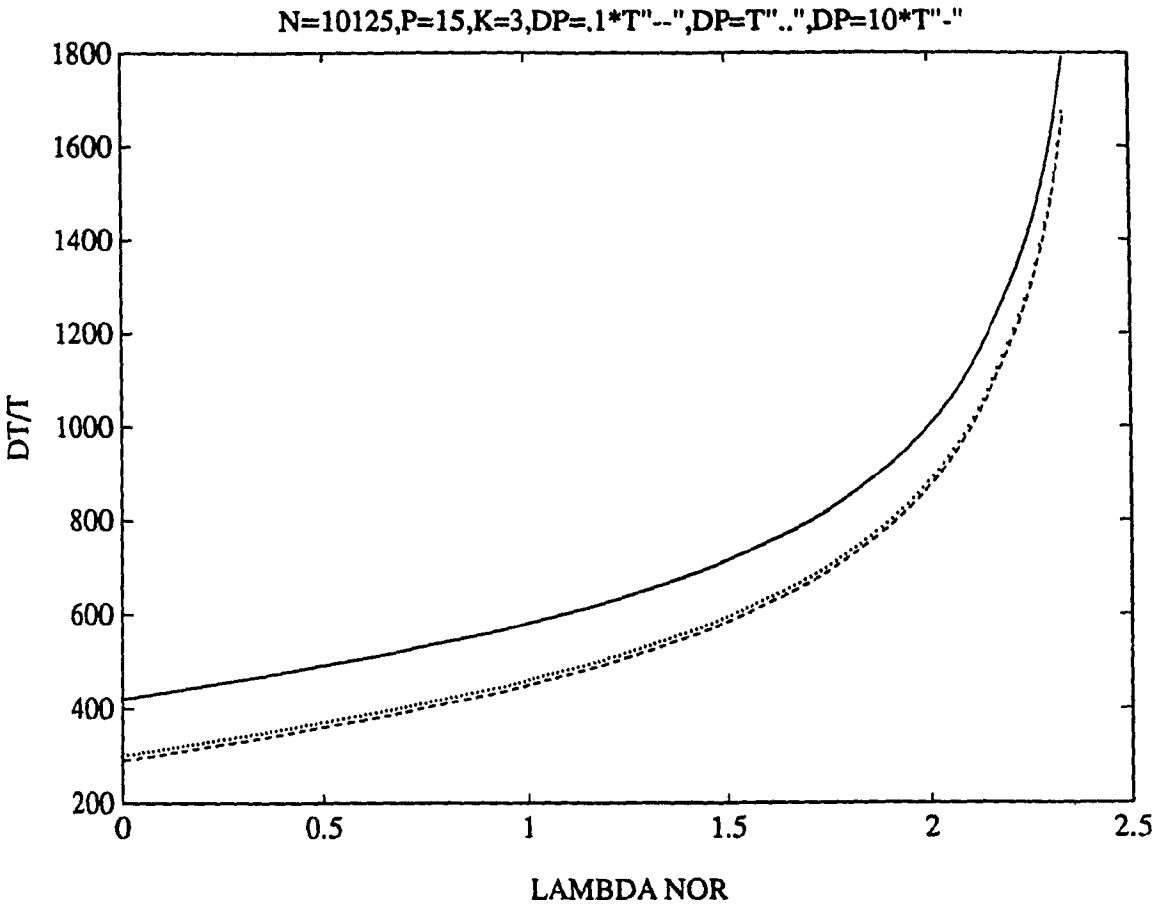

Figure 4.5. Performance Results as Function of D_p for the Case of N=10125, P=15, k=3.

For the same configuration there is a linear dependence between the total delay and the processing delay, because for the same configuration $D_1, D_2, \overline{H}$ and D_M remain constant.

For the second part the numerical results involve a comparison of the performance, in terms of message delay, for a range of connectivities and multiplexing factors. Four different sets of (P, k) are used, P varying from 2 to 15. For each set we get a different value of M, and for each set the processing delay is constant. The X-axis of Figures 4.6, 4.7, and 4.8 is λ_{NOR}, where λ_{NOR} is the traffic normalized to the level of traffic produced by 10000 stations for all 4 configurations. We obtained four different curves, and at each value of traffic load in the network we take the minimum value of the delay in the four cases. This gives us the optimum logical configuration. It is observed that as the traffic load increases we shift from one configuration to another, and the optimum configuration changes by changing the processing delay. Figure 4.6 shows the results for D_p =.1T, Figure 4.7 for the case of D_p =T, and finally Figure 4.8 shows the results for D_p = 10T.

The transformation from one configuration to another is effected by varying the connectivity P, which is the number of arcs from a station to the stations in the next column in the logical configuration (see Figure 3.1 and Table 3.1). The total traffic in the link is given by equation (4.8). As indicated, if λ and N are held constant, this total traffic decreases as P is increased. We define λ_{max} to be the maximum value of λ in equation (4.8). This is the traffic that would result in saturation of the optical links. Values of λmax as a function of P are shown in Table 4.1.

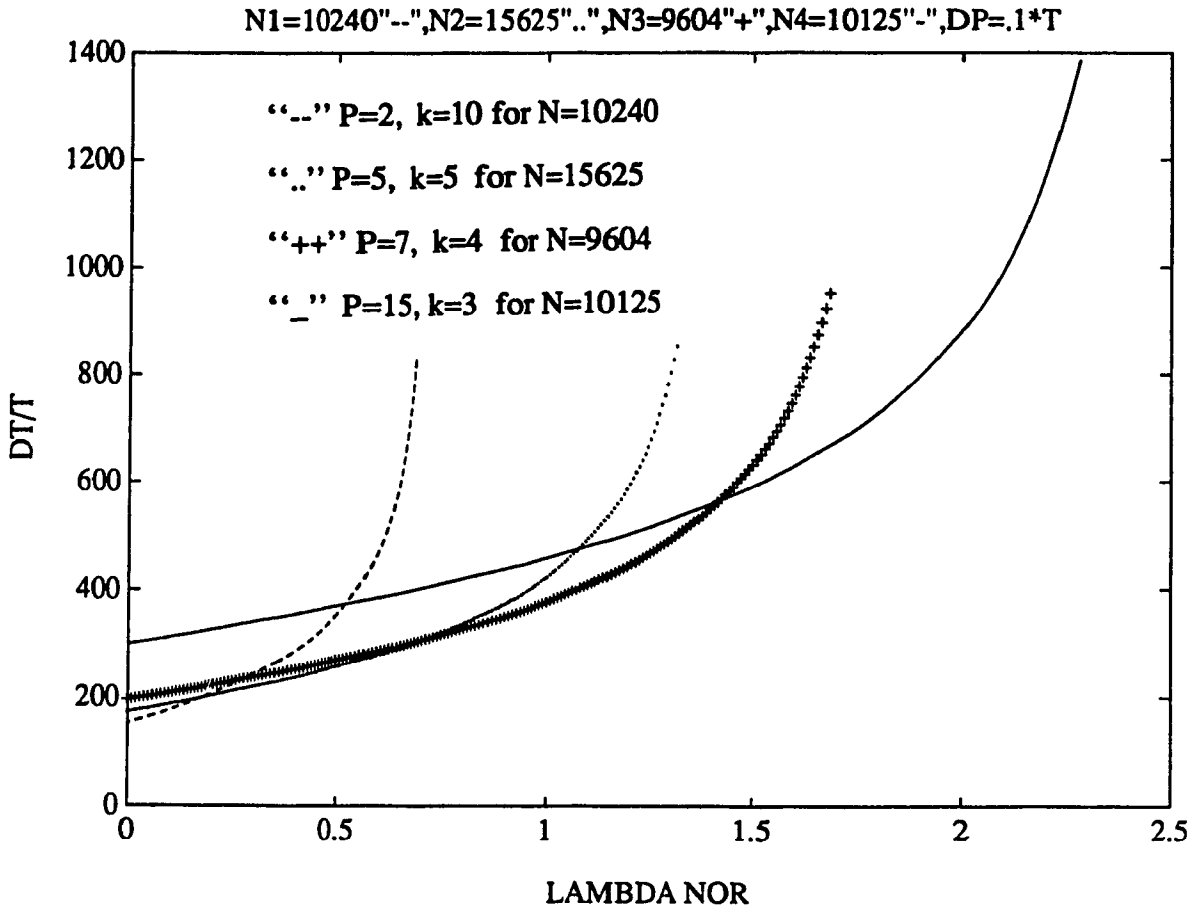

Figure 4.6. Performance Results for D_p = .1T

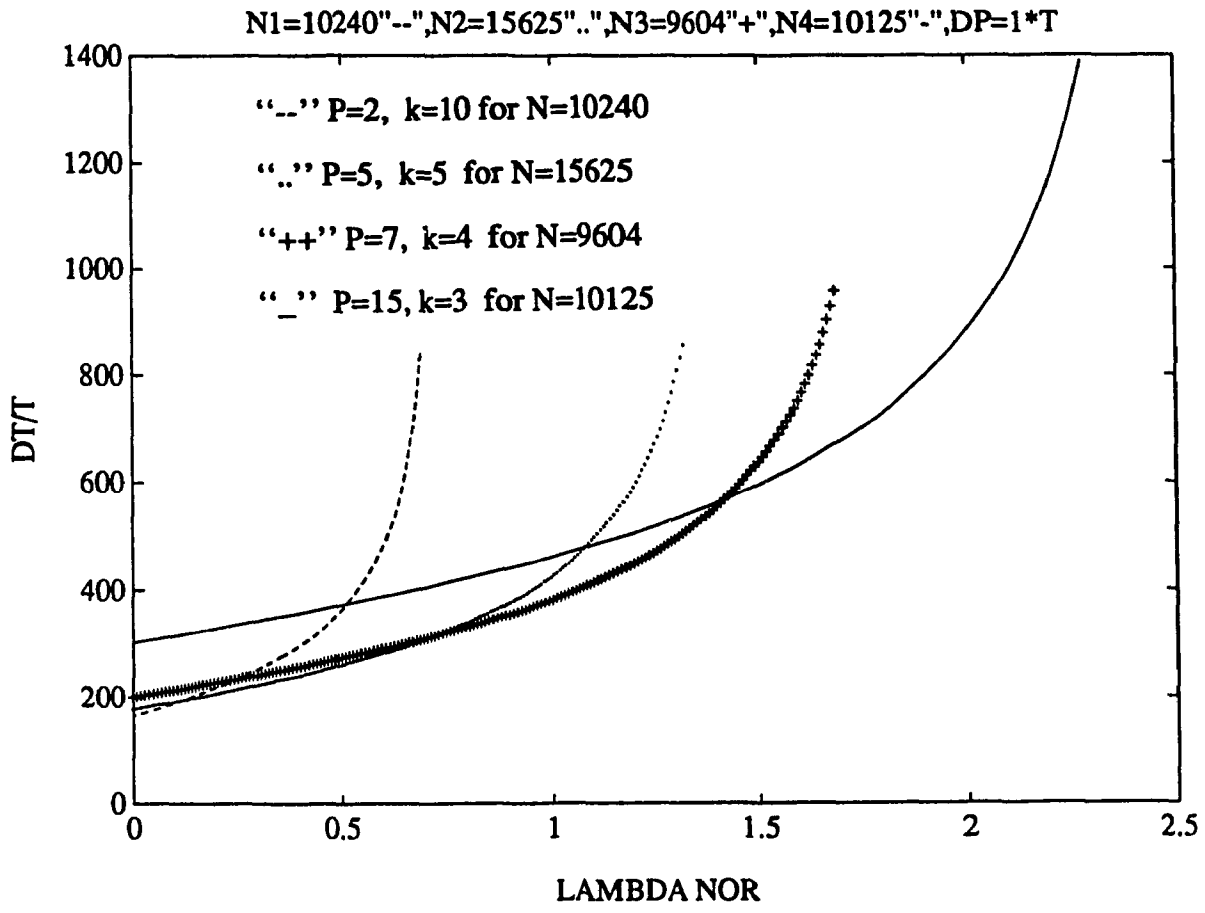

Figure 4.7. Performance Results for D_p = 1T

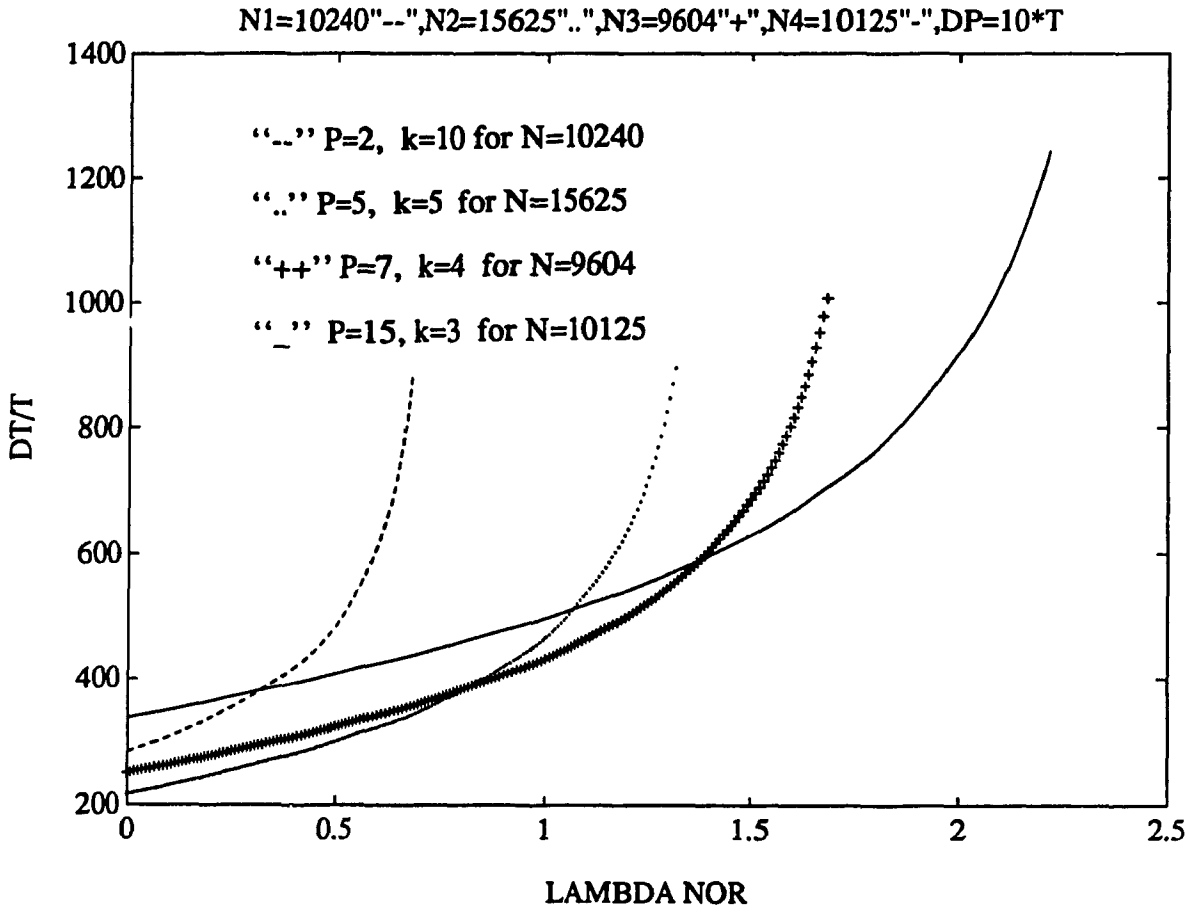

Figure 4.8. Performance Results for D_p = 10T

Table 4.1 The Maximum Traffic Load as Function of N, P, k.

N	P	k	λ_{max}
10240	2	10	0.72
15625	5	5	1.46
9604	7	4	1.87
10125	15	3	2.52

When we increase P this will reduce the number of hops $\overline{H}$. This is due to equation (3.5), which shows that to a first approximation, $\overline{H}$ is directly related to k, then by decreasing k, $\overline{H}$ is also decreasing. These results are shown in Table 4.2

Table 4.2 $\overline{H}$ as function of N, P, k.

N	P	k	$\overline{H}$
10240	2	10	13.5
15625	5	5	6.8
9604	7	4	5.3
10125	15	3	3.9

At the same time we have an increasing of the multiplexing factor. Due to the equation (3.20), M is directly related to P. By keeping N around 10,000 M increases as P increases. The effect of these two factors ($\overline{H}$ decreasing and M increasing)is an increase in the total delay.

CHAPTER FIVE

APPLICATION OF THE SHUFFLENET IDEA WHEN OPTICAL AMPLIFIERS ARE USED

In this chapter, we are interested in the application of the ShuffleNet idea when optical amplifiers are used in the physical topology. The ShuffleNet topology and operation are basically the same; however, there is a restriction on the number of stations that can be reached after a certain number of hops. The reason for this restriction is the limited number of users that can be reached through the same optical amplifier. Most the time this number is less than the logical number of users that can be reached at this given hop. Due to this limitation on the maximum number of users that can be reached through an optical amplifier, more hops are needed to cover all the users in the network.

5.1 The Physical Topology

The logical ShuffleNet structure is mapped into a given physical topology that connects several trees with a passive star through optical amplifiers at the input and the output of the passive star as described in chapter 3. When we discussed the case of optical amplifiers, we found a certain limitation on the bandwidth of the optical amplifiers. This will include a limitation of the number of wavelengths covered by optical amplifiers. This maximum number of wavelengths, denoted by Δ, is determined by the amplifier technology. In particular, this number is the ratio of the total range of the optical amplifier to the minimum channel spacing required to guarantee an acceptable crosstalk degradation. Given a channel bandwidth, B, the required channel spacing varies, practically, between 3 to 15 times (6 for the case of FDM, 15 for the case of WDM), depending on the modulation scheme. For example, if B = 1 GHz, a channel spacing of

6 B = 6 GHz, and a 10 nm optical bandwidth (1800 GHz at λ = 1.3 μm, or 1250 at λ = 1.5 μm) implies an amplifier capacity of 300 wavelengths at λ = 1.3 μm, and 208 wavelengths at λ = 1.5 μm. As a result of this study, different optical amplifiers will be used at different ranges to cover all the 1000 wavelengths used in our network. We may assume that we use F different amplifiers each of which can cover a certain number of different wavelengths. We assume all amplifiers have the same bandwidth and cover Δ wavelengths.

$$\Delta_1=\Delta_2=.....\Delta_F=\Delta \tag{5.1}$$

Then, the physical topology of the ShuffleNet can be represented as shown in Figure 5.1.

The total number of wavelengths available and used in the network is denoted by W. Then, the sum of the number of wavelengths covered by each amplifier should be equal to W.

$$W = \sum_{i=1}^{L} \Delta_i \tag{5.2}$$

Then the number of amplifiers needed to cover the band is

$$F = \left[\frac{W}{\Delta}\right]^{+} \tag{5.3}$$

One of the fundamental relations of the ShuffleNet structure is the total number of stations in the network, which is related to the number of columns and the number of links from each user. This relation is given by

$$N = kP^k \tag{5.4}$$

The N users are arranged in k columns, each containing P^k users. There are a total of PN logical links in the ShuffleNet. M is the multiplexing factor indicating the splitting of a wavelength to make up logical links.

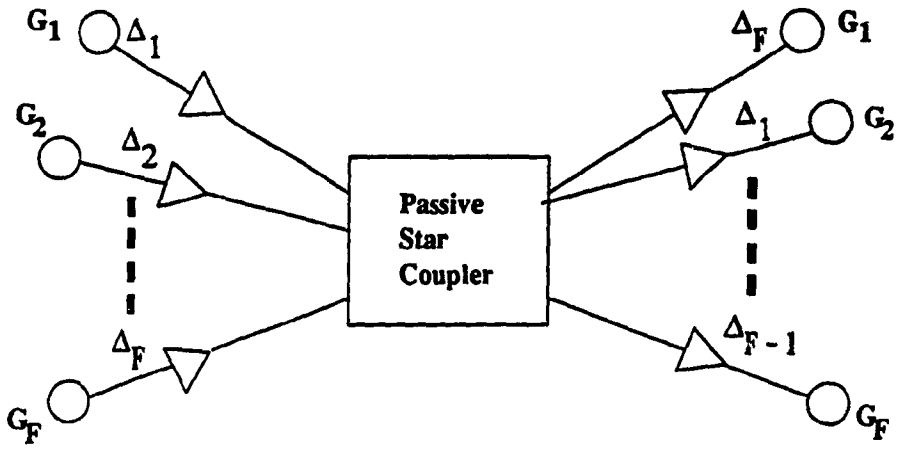

Figure 5.1. The Physical Topology of the ShuffleNet.

The relation between the total number of links and the multiplexing factor if there is a total of W wavelengths used in the network, is given by

$$MW \geq PN = kP^{k+1} \tag{5.5}$$

which means that the number of physical channels must be at least as large as the number of logical links.

We suppose that we have F different groups $G_1, G_2, \ldots, G_F$ where the members of a group sharing the same amplifier are based on a physical proximity. We also suppose that the number of members in each group is equal. Since the number of wavelengths covered by each group is equal to Δ, then the total number of physical channels available per group will be equal to Δ multiplied by the number of logical channels per wavelength which is equal to M. If every user transmits over P logical channels, then the number of users sharing the same group will be equal to the total number of logical channels per group divided by the number of logical channels per user. This is equal to $\frac{\Delta M}{P}$. If G denotes the maximum number of users that can share the same optical amplifier, by pure proportionality, we have

$$G = \frac{\Delta N}{W} \tag{5.6}$$

If there must be enough bandwidth for each member of the group to have its own logical connection, then we should have:

$$G \leq \frac{\Delta M}{P} \tag{5.7}$$

which from equation (6.6) and equation (6.7) reduces to

$$PN \leq MW \tag{5.8}$$

This is the same requirement as seen in equation (5.5). In addition, we have the requirement

$$\frac{P}{M} \leq \Delta \quad => \quad P \leq \Delta M \quad => \quad PN \leq N\Delta M \tag{5.9}$$

but the number of members of group sharing an amplifier is equal $\frac{N\Delta}{W}$. Since

$$\frac{N\Delta}{W} \geq 1 \quad \rightarrow \quad W \leq N\Delta \tag{5.10}$$

we have

$$W \leq N\Delta \tag{5.11}$$

Then, the complete relationship combining equation (5.5) and equation (5.11) is

$$PN \leq MW \leq \Delta NM \tag{5.12}$$

Since the same topology is used for the transmission side and the receiving side, then the same number of groups is used, and the bandwidth used for each amplifier is also the same, then the relations found above still hold. The number of members in the group is equal to:

$$G = \frac{N\Delta}{W} \tag{5.13}$$

and relation 5.12 still holds, which is

$$\frac{P}{M}\,\frac{N\Delta}{W} \leq \Delta \quad => \quad PN \leq MW \tag{5.14}$$

Then, we can conclude that there are enough receiving channels as long as (5.14) is satisfied, but this equation is the same as equation (5.5).

As the next step, we describe how the system will work under the limitation imposed by a limited bandwidth amplifier. First, recall that G denotes the number of stations sharing the same amplifier.

$$G = \frac{N\Delta}{W} \tag{5.15}$$

The system operates as described in chapter 4, with no limitation provided that

$$G \geq P \tag{5.16}$$

For example, if k=1, P=N (bus configuration) every station in the network transmits to all other stations and receives from all the others. In this particular case

$$G \geq N \tag{5.17}$$

This checks; we have only one group.

Now, let suppose that we have N, P, Δ, and W such that

$$P \leq G \quad => \quad P \leq \frac{N\Delta}{W} \tag{5.18}$$

Then we choose M such that (5.5) is satisfied, and we make the connections in a straightforward fashion. As an example we take the case of a ShuffleNet with N=24 stations arranged in 3 columns (k =3, and P=2).

For the ideal case given by Hluchyj and Karol [3] the unrestricted growth for a perfect ShuffleNet found in our previous study is given by

$$n(h) = \begin{cases} P^h & ;1 \leq h \leq k-1 \\ P^k - P^{(h-k)} & ;k \leq h \leq 2k-1 \end{cases} \tag{5.19}$$

Then for our special case we have: the first station in group 1 is connected to the first P stations (P=2) in group 2, these two stations in this group are connected to P^2=4 stations in group 3 as shown in Figure 5.2. In the next step these four stations are connected to (P^k-1)=7 stations in group 4. From this group we are connected to (P^k-P)=6 stations in group number 5. And finally from this group we are connected to (P^k-P^2)=4 stations in the last group, after this step we cover all stations in the network. This example is shown in Figure 5.3. We see that from each station in the network we can reach any other station after a maximum of 2k-1 hops. This is also equal to the maximum number of groups needed. These results are obtained with no condition on G, but G should be greater than

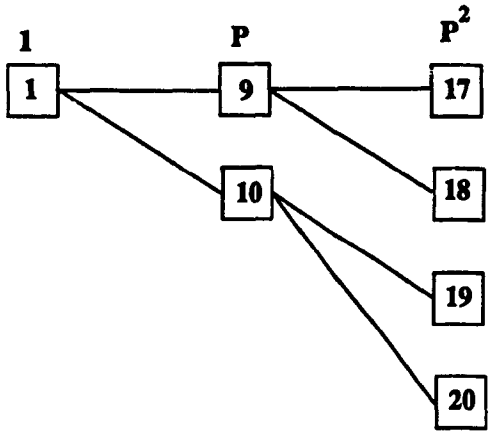

Figure 5.2. Tree Growth for the Case of P=2.

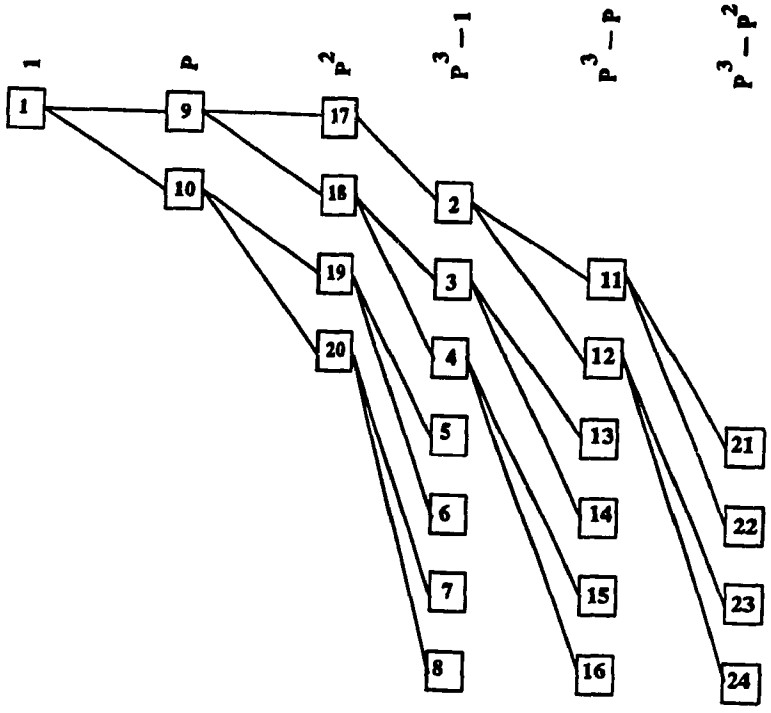

Figure 5.2. The ShuffleNet Connectivity Graph

N=24, P=2, k=3.

P^k-1 in the general case and equal to 7 in our particular example since each group cannot have more than P^k-1 members. Under this condition there is no modification of the results found by Hluchyj and Karol.

For the case where G is less than P^k-1, the connections are made modulo G since we must stay within the same wavelength group. This adds a significant restriction concerning the number of stations that can be reached after a given number of hops.
As a first step, we examine the effect of the restricted bandwidth on the particular example (N=24, P=2, k=3). If G ≥7, this corresponds to the ideal case where the size of the group is not more than 7. The connection graph is the same as the one shown in Figure 5.3 because still have the case of a perfect ShuffleNet. The maximum number of hops for this case is equal to 5.

When G=6, there is a restriction on the number of stations that can be reached. After the first hop we reach P=2 stations, and at the second hop another P^2=4 stations can be reached. At the third hop we are supposed to reach as many as P^3-1=7 stations but under the condition that G ≤6 only 6 stations can be reached. At the fourth hop we still reach P^3-P =6 stations, and at the fifth hop we can reach P^3-P^2=4 stations. If we make the total of stations reached after all five hops, only 22 stations are covered. since one station left to be reached, then another hop is needed to reach this station. Thus, under the condition of G=6, another hop must be added to reach all stations in the network, and the total number of hops has become equal to 6. The connection graph is shown in Figure 5.4. If the same example is studied for the case of G=5, at the third and the fourth hop only 5 stations can be reached at each hop instead of 7 at the third and 6 at the fourth. This will cause an addition of two hops; one to reach the two station missed at the third hop, and another one to reach the station missed at the fourth hop. This will increase the maximum number of hops required to reach all users by two and so that the hop count becomes equal to 7. The connection graph under this condition is shown in Figure 5.5. Figure 5.6 shows the connection graph for the case of G=4. The maximum

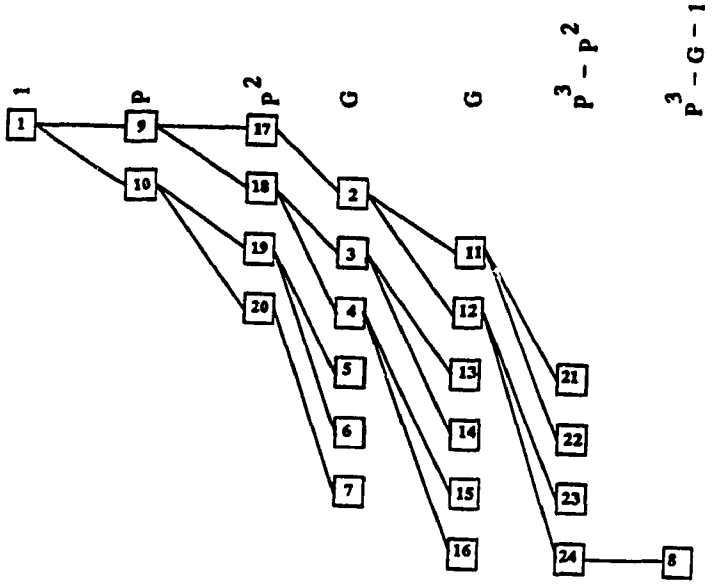

Figure 5.4. The Connectivity Graph for the Case of G=6

N=24, P=2, k=3.

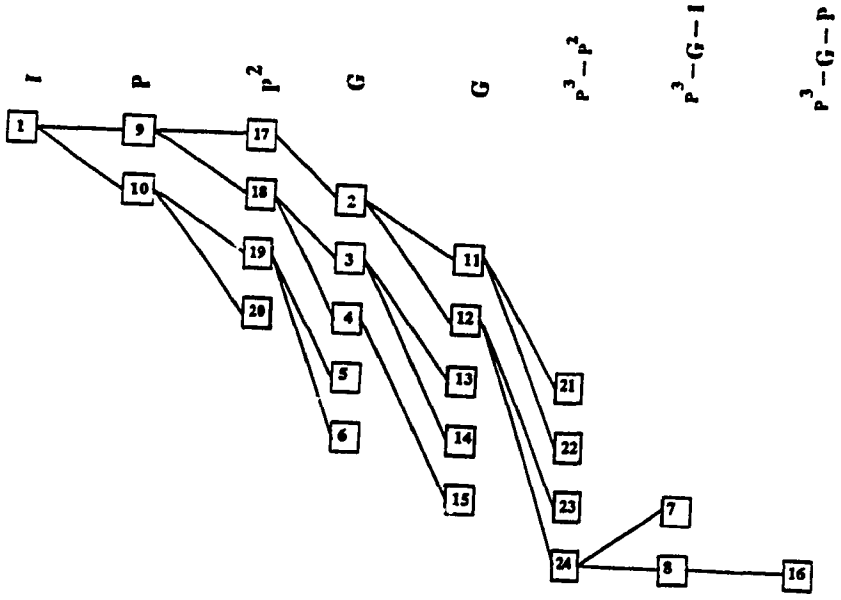

Figure 5.5. The Connectivity Graph for the Case of G=5

N=24, P=2, k=3.

number of hops for this case is equal to 7, as in the case of G=5, but the connection graph is not the same. Figure 5.7 shows the connection graph for the case of G=3, and the maximum number of hops required for this case is equal to 9. Figure 5.8 shows the connection graph for the case of G=2, and the maximum number of hops required for this case is equal to 12.

Having seen the effect of the bandwidth restriction on a particular case, we now present the general case of the spanning tree of the ShuffleNet; for a given G we find the maximum number of hops required to reach all stations in the network. As we mentioned before, if $G \geq P^k - 1$ the spanning tree is the same as the one given in Hluchyj and Karol paper (ideal case) but if $G < P^k - 1$, there is α such that

$$P^{\alpha} \leq G < P^{\alpha+1} - 1 \leq P^k - 1 \tag{5.20}$$

where $\alpha \leq k-1$. Starting from the first hop to the α^{th} hop the growth of the tree is as follows

$$P + P^2 + P^3 + \ldots\ldots + P^{\alpha-1} + P^{\alpha} \tag{5.21}$$

If α = k-1, at the k^{th} hop we can reach only G stations since $G \leq P^k - 1$, but if $\alpha < k-1$, then at the $(\alpha+1)^{th}$ we can reach only G stations since $G < P^{\alpha+1}$. Then for all subsequent hops until the k^{th} hop the spanning tree is as follows

$$G + G + \ldots\ldots + G \tag{5.22}$$

We note that at the k^{th} hop we return back to the first column to reach another G stations. But if $G > \frac{P^k - 1}{2}$ then we must pass through all columns to return back another time to the first column to reach all remaining stations. If $\frac{P^k - 1}{3} < G < \frac{P^k - 1}{2}$ then we must pass through all the columns twice to return back to the first column and reach the remaining stations.

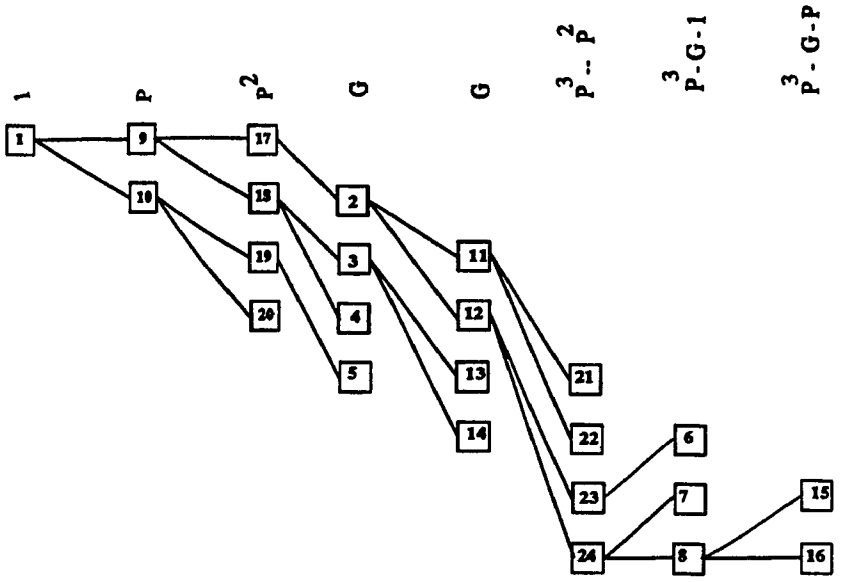

Figure 5.6. The Connectivity Graph for the Case of G=4.

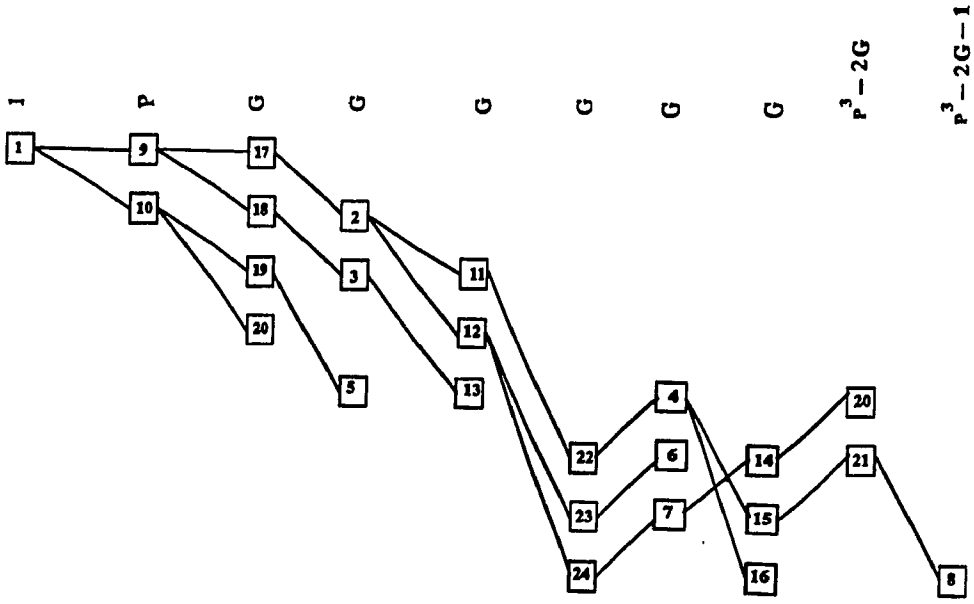

Figure 5.7. The Connectivity Graph for the Case of G=3.

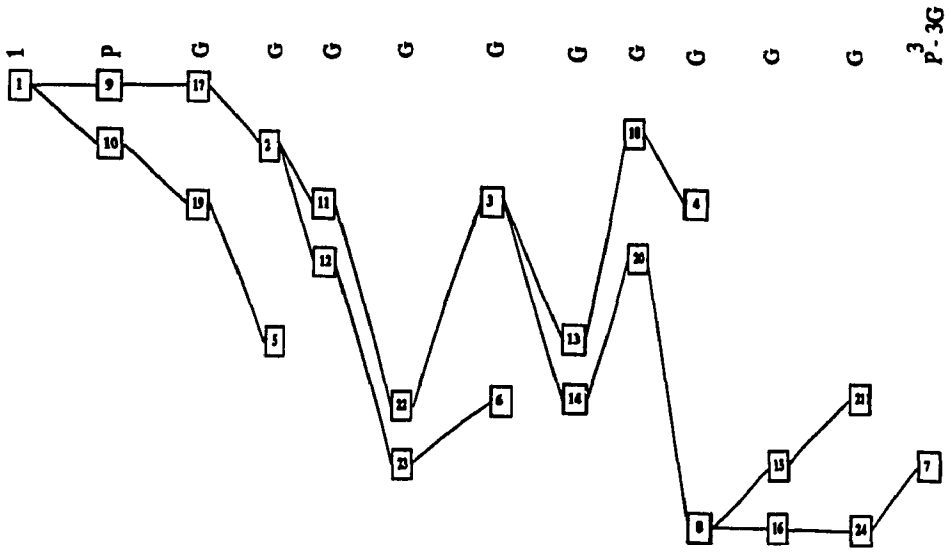

Figure 5.8. The Connectivity Graph for the Case of G=2.

In other words, we must make two tours through the network to return back to the first column, where a tour means passing through each column exactly one time. Then k hops are required at each tour before starting the next tour.

We now attempt to generalize these ideas to arbitrary G, P and k. Let Y denote the number of tours that are required to cover all stations in the first column. Y is given by

$$Y = \left[\frac{P^k - 1}{G}\right]^+ \tag{5.23}$$

where for the first (Y-1) tours we reach G stations in each tour and at the last tour we reach all of the remaining stations. Let R_1 denote the number of the remaining stations in the first column then

$$R_1 = P^k - 1 - (Y-1)\,G \tag{5.24}$$

After finding Y, we can derive the total number of hops required to reach all (N-1) stations in the network. As a first step, we go through (k-1) hops before starting the first tour. And as a second step we had to make (Y-1) tours before starting the last Y^{th} tour. Since each of the (Y-1) tours needs k hops then a total of (Y-1)k hops are made. Before starting the last tour, the total number of hops is equal to (Y-1)k+(k-1) = Y k - 1 hops. For the last step, we will find the total number of hops required for the last tour. This number is certainly less than k because our calculation of Y is based on a total of $(P^k - 1)$ stations not covered in the first column. Clearly, this is not true for the other column because we had reached P stations on the first hop, P^2 at the second hop, and so on until the α^{th} hop where we reached P^α stations. The number of the remaining stations per column will decrease when we go from the first column to the $(\alpha+1)^{th}$ column. Let R_i denote the number of the remaining stations in the $(i+1)^{th}$ column where $i \leq \alpha$

$$R_i = P^k - P^i - (Y-1)\,G \tag{5.25}$$

Going from the first column to the $(\alpha+1)^{th}$ column the number of the remaining stations

are decreasing until there are no more stations to reach. Let us suppose that at the $(\nu+1)^{th}$ column there are no more stations to reach, then the following relation holds

$$R_{\nu+1} \leq 0$$

$$P^k - P^\nu - (Y-1)\,G \leq 0 \tag{5.26}$$

This equation can be reduced to

$$P^\nu > P^k - (Y-1)\,G \tag{5.27}$$

We can use this relation to find the value of ν which will be equal to

$$\nu > \frac{log\,(P^k - (Y-1)\,G)}{log\,(P)} \tag{5.28}$$

Let ν^- equal to $[\nu]^-$ then we have

$$\nu^- = \left[\frac{log\,(P^k - (Y-1)\,G)}{log\,(P)}\right]^- \tag{5.29}$$

Given tht ν^- is less than ν then at the $(\nu^-+1)^{th}$ column the number of remaining stations is more than zero and at the $(\nu^-+2)^{th}$ column there are no stations left and no more hops are required. This means that the last tour has only (ν^-+1) hops. Finally the total number of hops required for all the network is equal to

$$Yk - 1 + \nu^- + 1 = Yk + \nu^-\ hops \tag{5.30}$$

Now, we show that, indeed, we have reached all stations in every column. Starting from the first column, Y steps are needed to cover all $P^k - 1$ stations. The first station is excluded because it is the transmitting station. In the first (Y-1) steps we cover G stations at each step. Finally at the Y^{th} step we cover all the remaining stations. The number of the remaining stations is equal to:

$$R_1 = P^k - 1 - (Y-1)\,G \tag{5.31}$$

For each of the remaining columns, P^k stations had to be reached. For the i^{th} column where $2 \le i \le \nu^- + 1$, (Y+1) steps are required, at the first step we cover P^{i-1} stations, for the following (Y-1) steps we cover G stations at each step, and finally at the last step we cover all remaining stations where the number is equal to:

$$R_i = P^k - P^{i-1} - (Y-1)\,G \tag{5.32}$$

for the j^{th} column where $\nu^- + 2 \le j \le \alpha + 1$, Y steps are needed. At the first step we cover P^{i-1} stations, for the following (Y-2) steps we cover G stations at each step, and finally at the last step we cover all remaining stations where the number is equal to:

$$R_j = P^k - P^{j-1} - (Y-2)\,G \tag{5.33}$$

For the l^{th} column where $\alpha + 2 \le l \le k$, we still need Y steps, at the first (Y-1) steps we cover G stations at each step, and finally for the last step we cover all remaining stations where the number is equal to:

$$R_l = P^k - (Y-1)\,G \tag{5.34}$$

In general for a (P, k) ShuffleNet, and for a given G, a spanning tree for assigning fixed routes to packets generated by any given user can be obtained, where:

h	Number of users h Hop from Source
1	P
2	P^2
.	.
.	.
.	.
$\alpha+1$	P^α
$\alpha+2$	G
.	.
.	.

.	.
k	G
.	.
.	.
.	.
(Y-1)k+v¯	G
(Y-1)k+v¯+1	$P^k-(Y-2)G-P^{v^-+1}$
.	.
.	.
(Y-1)k+α	$P^k-(Y-2)G-P^{\alpha}$
(Y-1)k+α+1	$P^k-(Y-1)G$
.	.
.	.
Yk-1	$P^k-(Y-1)G$
Yk	$P^k-(Y-1)G-1$
Yk+1	$P^k-(Y-1)G-P$
.	.
.	.
Yk+v¯	$P^k-(Y-1)G-P^{v^-}$

Those expressions can be reduced to the following equation, which relates the number of hops h to the number of users h hops from source $n(h)$

$$n(h)=\begin{cases} P^h & ;1\le h\le \alpha \\ G & ;(\alpha+1)\le h\le (Y-1)k+v^- \\ P^k-(Y-2)G-P^{(h-(Y-1)k)} & ;(Y-1)k+v^-+1\le h\le (Y-1)k+\alpha \quad (5.35) \\ P^k-(Y-1)G & ;(Y-1)k+\alpha+1\le h\le Yk-1 \\ P^k-(Y-1)G-P^{(h-Yk)} & ;Yk\le h\le Yk+v^- \end{cases}$$

This relation is the most important for the remaining part where we find the performance of the system under the restriction imposed by amplifier bandwidth.

5.2 Performance Calculation

5.2.1 Traffic Evaluation

For this part the traffic evaluation is made under the assumption of symmetric traffic. Then the traffic generated by one source can be represented as:

$$\Lambda' = \lambda \sum_{h=1}^{Yk+v^-} n(h)$$

$$= \lambda(N-1) \tag{5.36}$$

The total network bandwidth used by a single source is equal to:

$$B = \sum_{h=1}^{Yk+v^-} h\lambda(h)n(h) \tag{5.37}$$

For the symmetric case $\lambda(h)$ is constant for all h. Then B will be equal to:

$$B = \lambda \sum_{h=1}^{\alpha} hP^h$$

$$+ \lambda \sum_{h=\alpha+1}^{(Y-1)k+v^-} hG$$

$$+ \lambda \sum_{h=(Y-1)k+v^-+1}^{(Y-1)k+\alpha} h(P^k-(Y-2)G-P^{(h-(Y-1)k)})$$

$$+ \lambda \sum_{h=(Y-1)k+\alpha+1}^{Yk-1} H(P^k-(Y-1)G)$$

$$+\lambda \sum_{h=Yk}^{Yk+\nu^-} h(P^k-(Y-1)G-P^{(h-Yk)}) \tag{5.38}$$

From this equation we notice that B depends on α,ν^- and Y, but all of them are directly related to G. This equation can be evaluated numerically. For the expected value of h, $E[h]=\bar{H}$, this is equal to:

$$\bar{H} = \frac{\sum_{h=1}^{Yk+\nu^-} hn(h)}{\sum_{h=1}^{h=Yk+\nu^-} n(h)}$$

$$= \frac{B/\lambda}{\Lambda'/\lambda} = \frac{B}{\lambda(N-1)} \tag{5.39}$$

The total bandwidth used by all sources is equal to:

$$NB = kP^kB \quad bits / \sec \tag{5.40}$$

Since there are a total of kP^{k+1} links in the network; accordingly, each link must carry

$$\Lambda = \frac{kP^kB}{kP^{k+1}} = \frac{B}{P} \quad messages / \sec \tag{5.41}$$

This is the total amount of traffic on each link in the symmetric case. Of this Λ'/P is newly generated. If we go by the usual priority the locally generated traffic $\lambda(N-1)$ is split P ways for each output trunk:

$$\lambda_{local} = \frac{\lambda(kP^k - 1)}{P} = \frac{\lambda(N-1)}{P} \tag{5.42}$$

and the through traffic on a line is equal to :

$$\Lambda_T = \Lambda - \lambda_{local} \tag{5.43}$$

5.2.2 Delay Components

As in chapter 5, the sources of delay are queuing delay, multiplexing delay, and processing delay at the node. For each message we have two kind of queuing delay. The first queuing delay encountered by a message is when it enters the system; this is equal to D_2. At each subsequent hop an additional delay component is encountered, which is equal to D_1. For each hop we add the transmission delay T, the multiplexing delay D_M and the processing delay D_p. The expressions of D_1, D_2, D_M, and D_p are the same as those found in chapter 4. The total delay is given by

$$D_T = D_2 + D_1(\overline{H} - 1) + (T + D_M + D_p)\overline{H} \tag{5.44}$$

5.2.3 Numerical Results

To begin with, we are interested on the effect of the amplifier bandwidth Δ on the total delay. For the same configuration four different values of Δ are used. These results are shown in Figure 5.9 for the case when (N=10240, P=2, k=10), and Figure 5.10 for the case when (N=10125, P=15, k=3). These results show that when we decrease Δ the total delay increases. This is due to the increase of $\overline{H}$ as shown in Table 5.1, which is directly related to the maximum number of hops that increase by decreasing Δ.

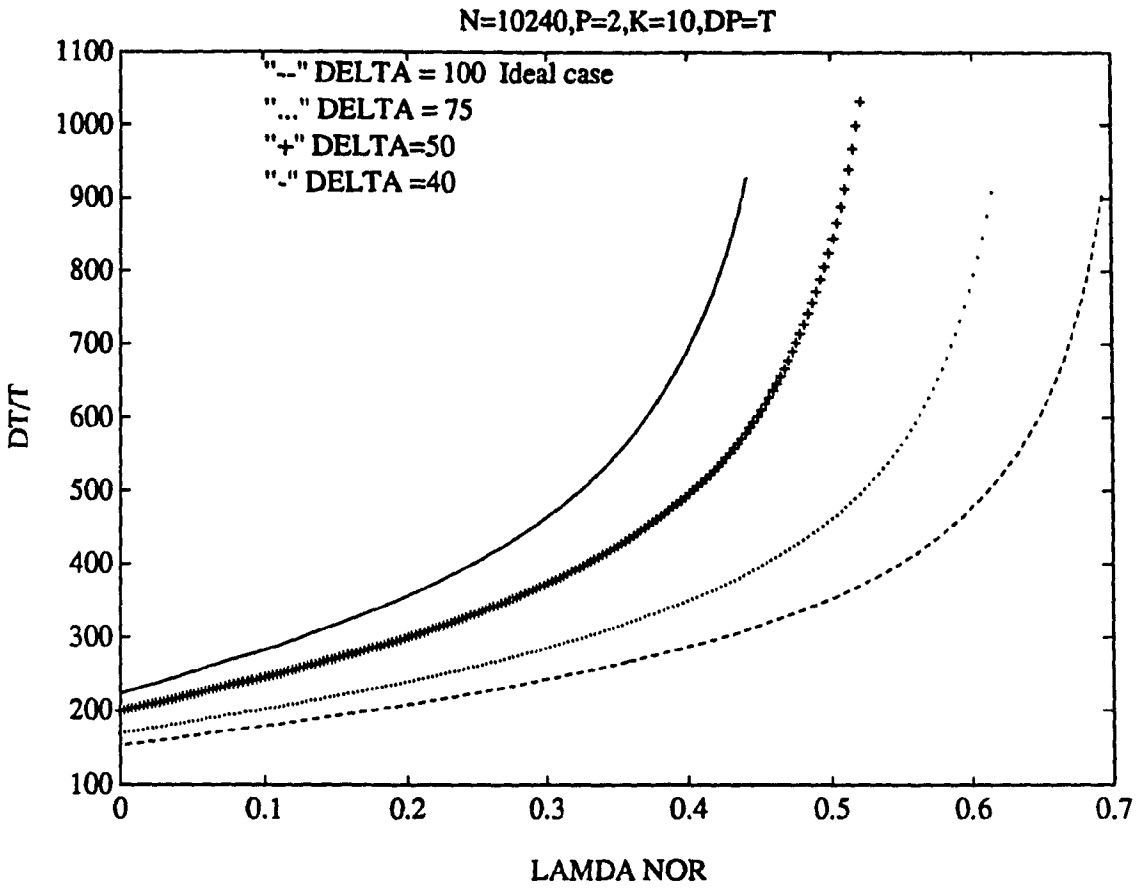

Figure 5.9. Performance Results as Function of Δ for the Case of N=10240, P=2, k=10.

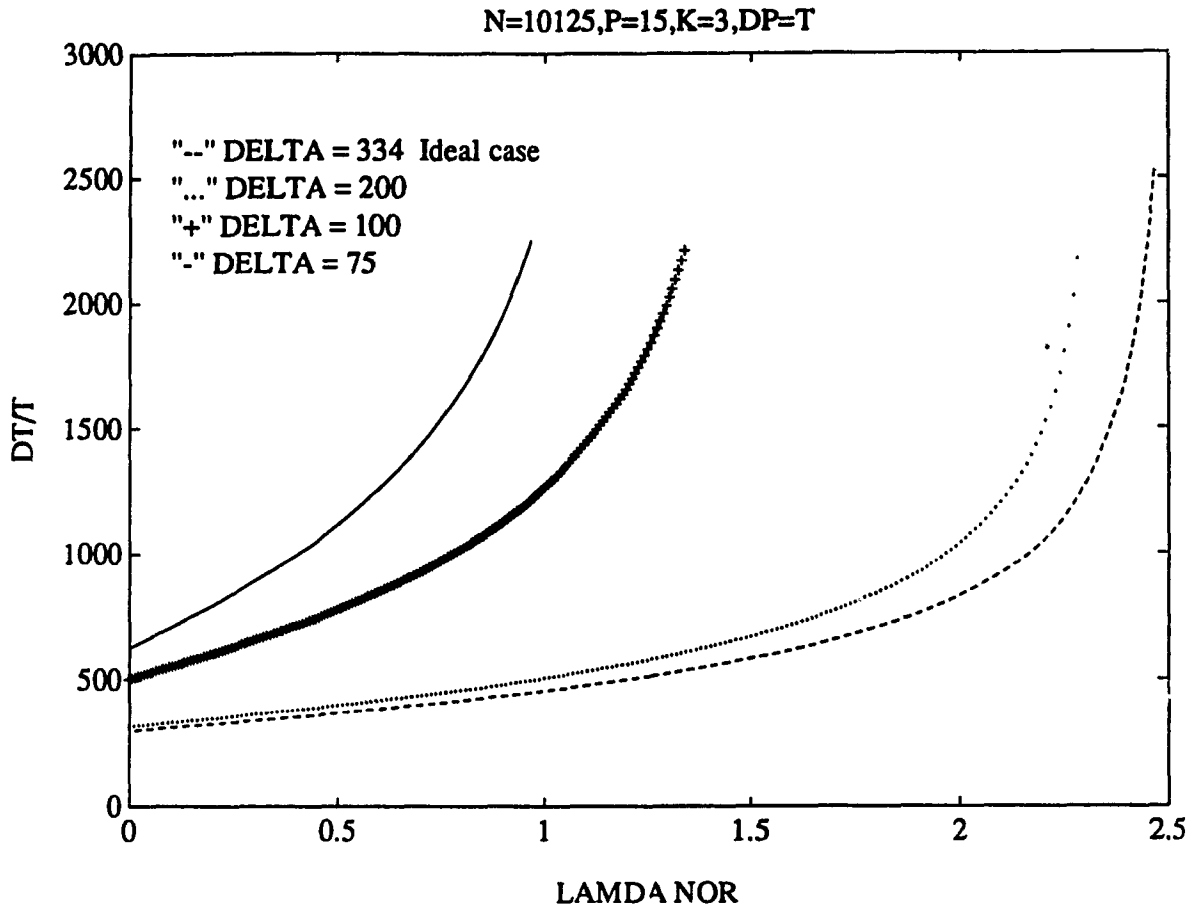

Figure 5.10. Performance Results as Function of Δ for the Case of N=10125, P=15, k=3.

Table 5.1 $\overline{H}$ as Function of Δ.

$\overline{H} = E[hops]$				
N	Δ≥334	Δ=200	Δ=100	Δ=75
10240	13.5	13.5	13.5	15.0
15625	6.8	6.8	8.4	10.2
9604	5.3	5.4	7.6	9.1
10125	3.9	4.1	6.6	8.2

At the same time we have a decreasing of the maximum traffic load λ as shown in Table 5.2, which is due to the restriction on the bandwidth of the optical amplifiers.

Table 5.2 The Maximum Traffic Load as Function of Δ

λ_{max}				
N	Δ≥334	Δ=200	Δ=100	Δ=75
10240	0.72	0.72	0.72	0.65
15625	1.46	1.46	1.17	0.96
9604	1.87	1.80	1.30	1.08
10125	2.53	2.37	1.51	1.21

Secondly the numerical results involve a comparison of the performance, in term of message delay, for a range of connectivity and multiplexing factor. Four different sets of (P, k) are used. P varies from 2 to 15; for each set we get a different value of M, and for each set the processing delay and Δ are the same. The X-axis of Figures 5.11, 5.12, and 5.13 is λ_{NOR}, where λ_{NOR} is the traffic normalized for the traffic produced by 10,000 equally active sources for all four configurations. We obtain four different curves, and at each value of traffic load in the network we take the minimum value of the delay in the four case. This gives us the optimum logical configuration under the same restriction of Δ. It is observed that as the traffic load increases we shift from one configuration to another. It also observed that the optimum configuration changes with changes in Δ. These results

are similar to those found in chapter 4, the only difference is when Δ decreases the effect of this is not similar for all configurations. For example the configuration with P = 15 is more affected than the one with P = 2. This is due to the fact that when G is closer to the total number of stations in each column (P^k), less modification is made compared to the original configuration. The E[hops] will increase faster and the effect of the bandwidth constraint is more evident.

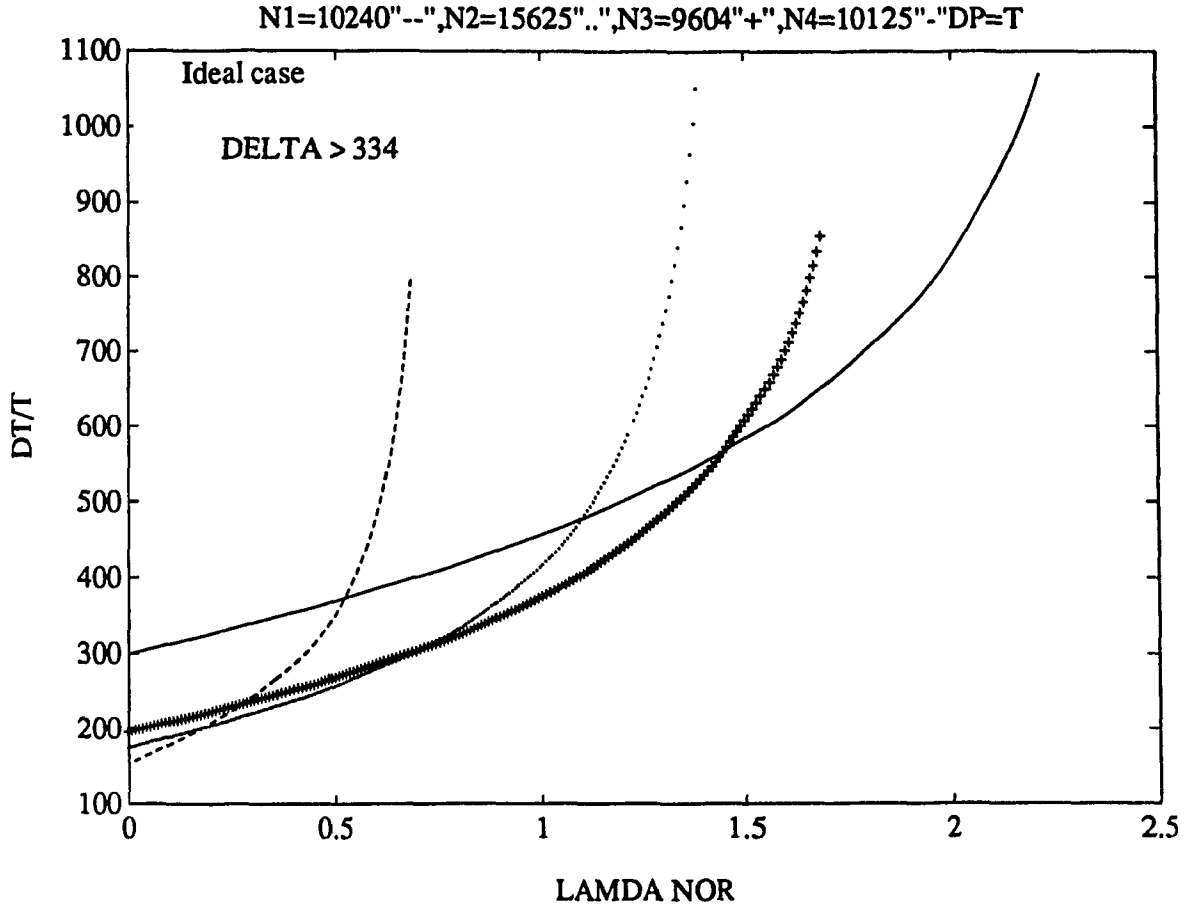

Figure 5.11. Performance Results when $\Delta \geq 334$

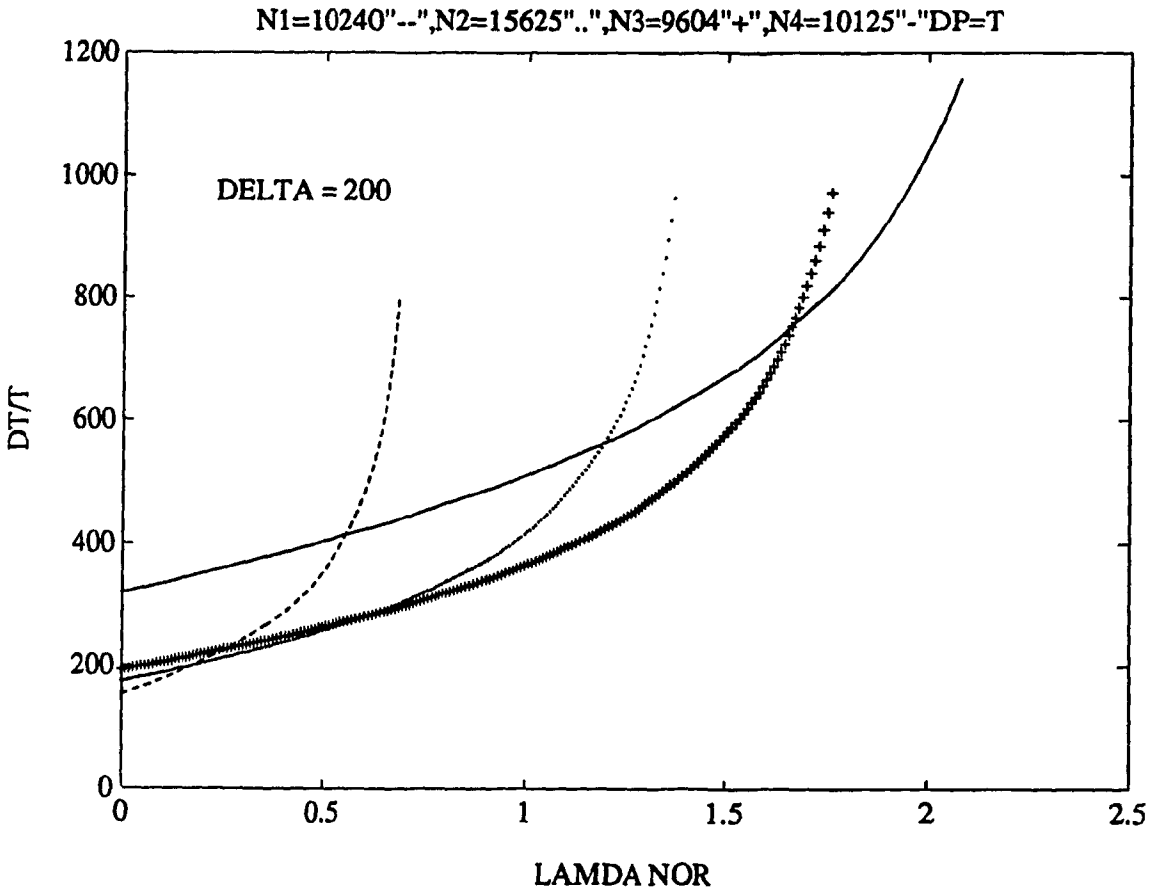

Figure 5.12. Performance Results when $\Delta = 200$

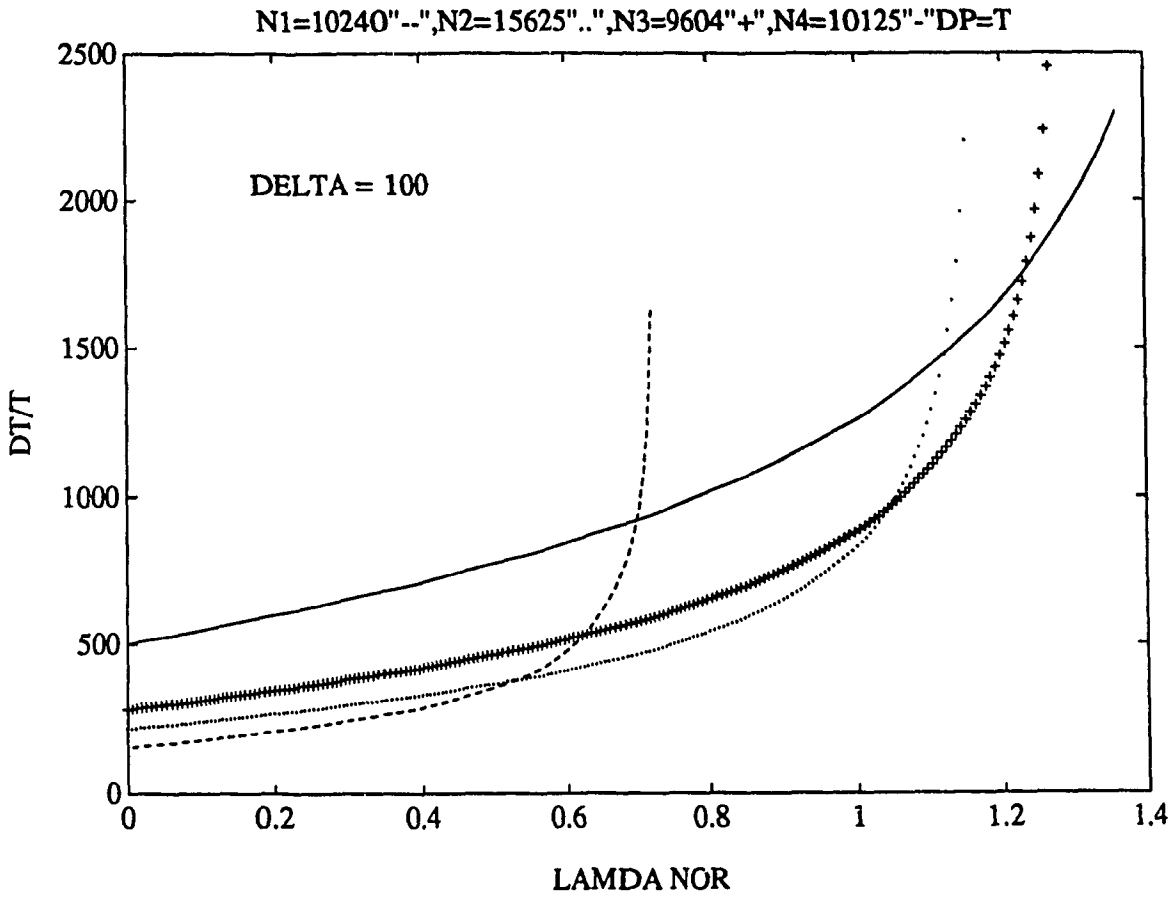

Figure 5.13. Performance Results when $\Delta = 100$

CHAPTER SIX

CONCLUSION

6.1 Conclusion

Following the introductory Chapter, in Chapter 2, the principles of propagation of optical energy, the transmission characteristics of optical fibers, and several optical components such us optical amplifiers and star couplers were discussed. This chapter also dealt with the principles of WDM, TDM, CDM, coherent and direct detection. In Chapter 3, a multichannel multihop lightwave network or ShuffleNet [3, 11] was presented. This topology is general in that it may assume one of a large range of forms, from a ring to a bus, by the control of a single parameter, the connectivity between stations. Several physical configurations are proposed for the physical implementation of this network. In chapter 4, a comparison of the performance in term of message delay, for a range of connectivities and multiplexing factors is made. In this chapter also an optimum logical configuration is provided as function of traffic load. Finally in chapter 5, the same comparison of the performance in term of message delay is made for the case when optical amplifiers are used. Optical amplifiers, by restricting bandwidth, limit the connections that can be made on a single hop. The optimum logical configuration is also provided for this case.

The analysis shows that ShuffleNet architecture insures an independence between the logical configuration and the physical topology used to support the network. The only limitation is the maximum number of stations that can be accommodated. The use of agile transmitters and receivers gives the ability to change the connectivity diagram among the nodes within the same physical topology. The use of optical amplifiers is the key component to increase the total number of station in the network. Thousand of

stations spread over a geographical region with a radius of up to 100 Km can be accommodated.

The performance criterion is in terms of message delay, for a range of connectivities and multiplexing factors. By taking the minimum value of the delay for each value of traffic load in the network, an optimum logical configuration is derived. As the traffic load increases we shift from one configuration to another. The increase of traffic load is compensated by an increase of connectivity between stations. The same analysis can be carried out for systems using optical amplifiers, taking into account a certain limitation due to the bandwidth of the optical amplifier. The bandwidth limits the number of channels that can be amplified. This causes an increasing in the total delay, and the optimum configuration is also modified.

The logical optimum configuration found can be adapted to a physical topology, and by using all necessary optical components, we can create the local optic adaptive distribution where the connectivity diagram among the nodes can be dynamically reconfigured as a function of the traffic load to insure the minimum delay in the network.

6.2 Suggestion for Further Research

The implementation of this local optic adaptive distribution involves the development of several optical components such as optical amplifiers which cause a certain limitation, and the fabrication of a NxN star coupler using a planar input waveguide array that radiates into a planar 'free-space' region where N is large. Only a 19x19 star coupler has been built using this method and all other suggestion are still theoretical or in the experimental stage. The direction of further research will involve the incorporation of these advances in technology into the network.

In our study we have considered pure perfect shuffle logical configurations where the number of stations is given by $N = kP^k$. Work needs to be done on more flexible archi-

tectures where the total number of stations is less rigidly defined by the connectivity.

The analysis has been carried out under the assumption of uniform traffic throughout the system. The effect of nonuniform traffic needs to be explored. We also need to examine architectures that adapt to nonuniform traffic as well as to a uniform increase in the traffic level.

REFERENCES

[1] S. E. Miller and I. P. Kaminow, "Optical Fiber Telecommunication II", New York: Academic Press, 1988.

[2] I. P. Kaminow, "Non-Coherent Photonic Frequency-Multiplexed Access Networks", *IEEE Network Magazine*, pp.4-10, March 1989.

[3] M. G. Hluchyj and M. J. Karol, "ShuffleNet: An Application of Generalized Perfect Shuffles to Multihop Lighwave Networks", *IEEE Trans.Commun.*, 1988.

[4] A. A. M. Saleh and H. Kogelnik, "Reflective Single-Mode Fiber-Optic Passive Star Couplers", *J.Lightwave Technol*, March 1988.

[5] C. Dragone, "Efficient NxN Star Coupler Based on Fourier Optics", *Electron.Lett.*, vol.24, no.15, pp.942-944,1988.

[6] C. Dragone, private communication.

[7] M. Gerla and L. Fratta, "Tree Structured Fiber Optic MAN's", *IEEE J.Selec.Areas Commun.*, vol.6, no.6, July 1988.

[8] D. Towsley, "The Analysis of a Statistical Multiplexer with Nonindepedent Arrivals and Errors", *IEEE Trans.Commun*, vol.COM-28, no.1, Jannuary 1980.

[9] J. F. Hayes, "Modeling and Analysis of Computer Communication Networks", Plenum Press. New York and London, 1984.

[10] M. J Karol and S. Shaikh, "A Simple Adaptative Routing Scheme for ShuffleNet Multihop Lightwave Networks", *GLOBCOM'88 Conf. Rec.*, pp.1640-1647, November 1988.

[11] A. S. Acampora, "A Multichannel Multihop Local Lightwave Network", *GLOBECOM'87 Conf. Rec.*, pp.1459-1467, November 1987.

[12] M. M. Nassehi, F. A. Tobagi, and M. E. Marhic, "Fiber Optic Configuration for

Local Area Networks", *IEEE J.Selec.Area Commun.*, vol.3, no.6, November 1985.

[13] K. T. Ko, and B. R. Davis, "Delay Analysis for a TDMA Channel with Contignous Output and Poisson Message Arrival", *IEEE Trans.Commun.* vol. Com-32, no.6, June 1984.

[14] M. Eisengerg, and N. Mehravari, "Performance of the Multihop Lightwave Network Under Nonuniform Traffic", *IEEE J.Selec.Areas.Commun*, vol.6, no. 7, August 1988.

[15] E. Rocher, "Application of Monomode Fiber to Local Networks", *IEEE J.Selec.Areas.Commun.*, vol. Sac3, no.6, November 1985.

[16] G. J. Foschini and A. A. M. Saleh, "Overcoming Optical Amplifier Intermodulation Distortion Using Coding in Multichannel Communication Systems", *IEEE Trans.Commun.*, vol.38, no.2, February 1990.

[17] R. A. Linke, "Frequency Division Multiplexed Optical Networks Using Heterodyne Detection", *IEEE Network*, March 1989.

[18] J. M. Senior,"Optic Fiber Communications Principles and Practice", Prentice Hall,1985.

[19] Technical Staff of CSELT, "Optical Fiber Communications",McGraw Hill Book Company, 1980.

[20] G. Keiser, "Optical Fiber Communications", McGraw Hill Book Company, 1983.

[21] J. C. Palais, "Fiber Optic Communications", Prentice Hall, Inc., 1984.

[22] P. S. Henry, "High-Capacity Lightwave Local Area Networks", *IEEE Commun.Mag.*, vol.27, no.10, October 1989.

[23] S. D. Personic, "Optical Fiber Transmission System", *Springer Series in Solid-State Sciences*, Springer Verlag, vol.39, 1980.

[24] H. Kressel, "Semiconductor Devices for Optical Communication", *Springer Series in Solid-State Sciences,* Springer Verlag, vol.39, 1980.

[25] G. Keiser, "Optical Fiber Communications", McGraw Hill Book Company, 1983.

[26] M. W. Fleming and A. Moordian, "Fundamental Line Broadening of Single-Mode GaAlAs Lasers", *Appl.Phys.Lett.*, vol.38, 1981.

[27] H. Kobrinski and K. Cheung, "Wavelength-Tunable Optical Filters: Applications and Technologies", *IEEE Commun.Mag.*, vol.27, no.10, October 1989.

[28] J. Salz, "Modulation and Detection for Coherent Lightwave Communications", *IEEE Commun.Mag.*, vol.24, no.6, June 1986.

[29] S. T. Personick, "Fiber Optics Technology and Applications", *AT&T Technical Journal,* vol.66, Jan./Feb. 1987.

[30] Motorola Inc., "Optoelectronics Device Data", 1983.

[31] T. P. Lee and C. Zah, "Wavelength-Tunable and Single-Frequency Semiconductor Lasers for Photonic Communications Network", *IEEE Commmu.Mag.*, vol.27, no.10, October 1989.

[32] J. A. Bannister, L. Fratta and M. Gerla, "Topology Design of Wavelength-Division Optical Network", *IEEE Infocom'90*, vol.3, June 1990.

APPENDIX A

THE EXPECTED QUEUE LENGTH

FOR THE LOWER PRIORITY PACKETS

In this part, we focus our study on the lower priority packets. The low priority view a system which periodically breaks down (the breakdown is due to servicing of high priority packets). The time between breakdown periods corresponds to the busy period for the low priority packets because during this period there are no high priority packets and the system can serve the low priority packets. The duration of the breakdown period corresponds to the busy period for the high priority packets because during this period the system is interrupted to serve high priority packets.

Let us assume that $G_{(c)}(z)$ is the generating function for the distribution of the number of class c packets arriving in a slot, $c=1,2$. The parameters of the breakdown model given by the Towsley paper [7] take the following form:

r: the probability of having no class one messages in a slot.

$r=G_{(1)}(0)$

$\bar{r}=1-r$

$B(z)$ is the generating function for the busy period distribution for high priority packets, and it is given by:

$$B(z)=\frac{G_{(1)}[z(r+(1-r)B(z))]-r}{1-r} \qquad \text{(A.1)}$$

Finally the expected queue length of the low priority packets is equal to:

$$E[L] = G_D'(1) + \frac{G_D''(1)}{r(1-G_D'(1))}$$

$$+\frac{\bar{r}B'(1)}{1+\bar{r}B'(1)}G_{(2)}'(1)(B''(1)+B'(1))/2B'(1) \qquad (A.2)$$

Where

$$G_D(z)=G_{(2)}(z)[r+\bar{r}B(G_{(2)}(z))] \qquad (A.3)$$

And

$$G_D'(1)=\frac{\partial G_D(z)}{\partial z}\Big|_{z=1}$$

$$=G_{(2)}'(z)(r+\bar{r}B(G_{(2)}(z))$$

$$+G_{(2)}(z)(\bar{r}G_{(2)}'(z)B'(G_{(2)}(z))\Big|_{z=1}$$

$$=G_{(2)}'(1)(r+\bar{r}B(1))+(\bar{r}G_{(2)}(1)B'(1))$$

$$=G_{(2)}'(1)+(\bar{r}G_{(2)}'(1)B'(1))$$

$$=G_{(2)}(1)[1+\bar{r}B'(1)] \qquad (A.4)$$

$$G_D''(1)=\frac{\partial^2 G_D(z)}{\partial z^2}\Big|_{z=1}$$

$$=G_{(2)}''(z)(r+\bar{r}B(G_{(2)}(z))+2(G_2'(z))^2\bar{r}B'(G_{(2)}(z))$$

$$+G_{(2)}(z)[\bar{r}G_{(2)}''(z)B'(G_{(2)}(z))$$

$$+\bar{r}(G_{(2)}'(z))^2 B''(G_{(2)}(z))]\,|_{z=1}$$

$$=G_{(2)}''(1)+2[G_{(2)}(1)]^2\bar{r}B'(1)$$

$$+\bar{r}[G_{(2)}''(1)B'(1)+(G_{(2)}'(1))^2 B''(1)] \qquad \text{(A.5)}$$

Given that

$$B(z)=\frac{G_{(1)}[z(r+\bar{r}B(z)]-r}{1-r} \qquad \text{(A.6)}$$

Then

$$B'(1)=\frac{\partial B(z)}{\partial z}\,|_{z=1}$$

$$=\frac{[(r+(1-r)B(z))+z(1-r)B'(z)]G_{(1)}(z(r+(1-r)B(z)))}{1-r}\,|_{z=1}$$

$$=\frac{[1+(1-r)B'(1)]G_{(1)}'(1)}{1-r}$$

$$=\frac{G_{(1)}'(1)}{1-r}+B'(1)G_{(1)}'(1)$$

$$=\frac{G_{(1)}'(1)}{(1-r)(1-G_{(1)}'(1))} \qquad \text{(A.7)}$$

$$B''(1)=\frac{\partial^2 B(z)}{\partial z^2}\,|_{z=1}$$

$$=\frac{1}{1-r}\left[[2(1-r)B'(1)+(1-r)B''(1)]G_{(1)}'(1)\right]$$

$$+[1+(1-r)B'(1)]^2 G_{(1)}''(1) \tag{A.8}$$

If we take all $B''(1)$ to the left side our equation becomes:

$$B''(1)=\frac{2B'(1)G_{(1)}'(1)}{(1-G_{(1)}'(1))}+\frac{[1+(1-r)B'(1)]^2 G_{(1)}''(1)}{(1-r)(1-G_{(1)}'(1))} \tag{A.9}$$

If we substitute the value of $B'(1)$ in the equation we get

$$B''(1)=\frac{2[G_{(1)}'(1)]^2}{(1-r)(1-G_{(1)}'(1))^2}+\frac{G_{(1)}''(1)}{(1-r)(1-G_{(1)}'(1))^3} \tag{A.10}$$

The substitution of equation (A.7), (A.10), in equation (A.4), (A.5) gives:

$$G_D'(1)=G_{(2)}'(1)[1+\frac{G_{(1)}'(1)}{1-G_{(1)}'(1)}]$$

$$=\frac{G_{(2)}'(1)}{1-G_{(1)}'(1)} \tag{A.11}$$

$$G_D''(1)=G_{(2)}''(1)+2(G_{(2)}'(1))^2\frac{G_{(1)}'(1)}{1-G_{(1)}'(1)}$$

$$+G_{(2)}''(1)\frac{G_{(1)}'(1)}{1-G_{(1)}'(1)}+(G_{(2)}'(1))^2\frac{2(G_{(1)}'(1))^2}{(1-G_{(1)}'(1))^2}$$

$$+(G_{(2)}'(1))^2\frac{G_{(1)}''(1)}{(1-G_{(1)}'(1))^3}$$

$$=\frac{G_{(2)}''(1)+2(G_{(2)}'(1))^2 G_{(1)}'(1)}{1-G_{(1)}'(1)}$$

$$+\frac{(G_{(2)}'(1))^2[2G_{(1)}'(1)-2(G_{(1)}'(1))^3+G_{(1)}''(1)]}{2[1-G_{(1)}'(1)]^2[1-G_{(1)}'(1)-G_{(2)}'(1)]} \tag{A.12}$$

Now let us find the other terms in equation (A.2)

First term:

$$\frac{G_D''(1)}{2(1-G_D(1))}=\frac{G_{(2)}''(1)+2(G_{(2)}'(1))G_{(1)}'(1)(1-G_{(1)}'(1))}{2[1-G_{(1)}'(1)][1-G_{(1)}'(1)-G_{(2)}'(1)]}$$

$$+\frac{(G_{(2)}'(1))^2[2G_{(1)}'(1)-2(G_{(1)}'(1))^3+G_{(1)}''(1)]}{2[1-G_{(1)}(1)]^2[1-G_{(1)}'(1)-G_{(2)}'(1)]} \tag{A.13}$$

Second term:

$$\frac{rB'(1)}{1-\bar{r}B'(1)}\frac{G_{(2)}'(1)(B''(1)+B'(1))}{2B'(1)}=$$

$$\frac{G_{(2)}'(1)[G_{(1)}'(1)]^2}{1-G_{(1)}'(1)}+\frac{G_{(2)}'(1)G_{(1)}''(1)}{2[1-G_{(1)}'(1)]^2} \tag{A.14}$$

The substitution of the equations (A.11), (A.12), (A.13), (A.14), in equation (A.2) gives us the expected queue length $E[L]$ as a function of $G_{(1)}(z)$ and $G_{(2)}(z)$. Finally the expected queue length of the low priority packets is given by:

$$E[L]=G_{(2)}'(1)[1-G_{(1)}'(1)]+\frac{G_{(2)}''(1)+4G_{(2)}'(1)[G_{(1)}'(1)]^2}{2[1-G_{(1)}'(1)-G_{(2)}'(1)]}$$

$$+\frac{G_{(1)}''(1)G_{(2)}'(1)}{2[1-G_{(1)}'(1)][1-G_{(1)}'(1)-G_{(2)}'(1)]} \tag{A.15}$$